Fluorescently Labeled Sodium Hyaluronate:
Synthesis, Characterization and Solution Properties

Fluorescently Labeled Sodium Hyaluronate: Synthesis, Characterization and Solution Properties

by
Kimberley D. MacEwan Gracie, B.Sc.

A Thesis Submitted to the School of Graduate Studies
in Partial Fulfillment of the Requirements for the
Degree of Masters of Science

McMaster University

MASTER OF SCIENCE (1998)
(Chemistry)

MCMASTER UNIVERSITY
Hamilton, Ontario

TITLE: **Fluorescently Labeled Sodium Hyaluronate:** Synthesis, Characterization and Solution Properties

AUTHOR: Kimberley D MacEwan Gracie
(St. Francis Xavier University,
Antigonish, Nova Scotia)

SUPERVISOR: Dr. F.M. Winnik

NUMBER OF PAGES: 92

Abstract

Fluorescence spectroscopy has been proven to be a useful technique for the investigation of the structural, physical and solution properties of polymers. A polymer system containing a photo physical probe can be investigated using fluorescence quenching and polarization. We have randomly labeled sodium hyaluronate (HA) chains with fluorescent dyes such as 1-(1-pyrenyl)methyl amine and N-ε-dansyl-L-lysine, and studied their physical, structural and solution properties, including interactions with surfactants using the above fluorescence techniques.

Acknowledgments

Firstly, I would like to thank my two children, Jillian Dawn and Jamie Natashia, for all their love, support and encouragement over the years.

I would like to thank Fadi H. Asfour for all his help, encouragement and love over the past two years. Also, thanks to Randy Frank and Jeff Downey for simply providing a place to hide...thanks guys!

I would like to thank Dr. Winnik for allowing me the opportunity to finish my masters.

I would like to thank all the people in my lab group namely, Jing Zhang, Sudarshi Regismond, Jean-Francois Strumbe and Ming Li.

I would like to thank the following people who have contributed to my thesis:

Dr. Pierre Brassard, for helping me build a double junction reference electrode,

Dr. McGlinchey, for listening to all my complaints and just being there,

Carol Dada and the entire Chemistry Department Staff

Dr. Willie Leigh, for all his kindnesses and an awesome reference letter. Last, but most certainly not least, I would like to thank my mother Carol MacEwan for all the help and care she has given me and my children during my educational pursuits.....thanks mom.

Dedication

I would like to dedicate my thesis to my two beautiful children, Jillian Dawn and Jamie Natashia. Girls, thanks for loving and support mommy for the past six years of my educational pursuit. We did it VEE VEE ~_^

TABLE OF CONTENTS

List of Figures

List of Tables

List of Schemes

List of Abbreviations

Hyaluronic Acid	HA
1-(1-Pyrenyl)methyl amine	PMA
N-ε-Dansyl-L-Lysine	DL
1-(1-Pyrenyl)carboxyaldehyde	PCA
Labeled HA is represented by a dash	HA-DL
	HA-PMA
Probed solutions of HA represented by a slash	HA/DL
	HA/PMA
	HA/PCA
Cetylpyridinium Chloride	CPC
Dodecylpyridinium Chloride	DoPC
Ethylpyridinium Bromide	EtPyBr
Poly(N-ethyl-4-vinylpyridinium) Bromide	VEPBr
Dodecyltrimethylammonium Bromide	DTAB
Tetradecyltrimethylamminium Bromide	TTAB
Hexadecyltrimethylammonium Chloride	HTAC
Critical micellar concentration	CMC
Critical aggregation concentration	CAC

1. Introduction

1.1 Hyaluronic Acid

Karl Meyer was the first to report the isolation of hyaluronic acid, HA, from the vitreous body of the eye.[1] He named the compound "hyaluronan" from hyaloid meaning vitreous and uronic acid. In its biological form, HA exists as highly viscous solutions and is a neutral salt.[1] It occurs as salts of alkaline earth cations, in particular Na^+, K^+, Ca^{2+}, or Mg^{2+}.[2]

Hyaluronan acts as a molecular filter,[2,3] shock absorber,[3,4] and support structure for collagen fibrils.[3,5] Hyaluronan is found throughout the extracellular matrix of all higher animals, with the highest concentrations found in soft connective tissues. The polymer has been isolated from joint fluid,[4] rooster combs,[5] bovine eyes,[1] umbilical cords.[4,5] It has also been produced by streptococci.[5] Most commercial HA is extracted from the posterior-peripheral and central vitreous region of adult bovine eyes, or from rooster combs. It is purified by ultracentrifugation to remove any water insoluble constituents. Proteins are removed by *pronase* digestion.[5] The molecular weight of HA varies greatly depending on the source. It ranges from 1.4×10^7 daltons, in synovial fluid, to 77, 000 daltons for a fraction of vitreous body.

The applications of HA include ophthalmology, rheumatology, traumatology to

cosmetics and dermatology .[4]

1.1.1 Chemical Structure of Hyaluronic Acid

The primary structure of HA was established by Meyer and co-workers in the 1950's.[6] They found, through chemical and enzymatic digestion, that the HA backbone was a linear polysaccharide consisting of two sugars: β-D-glucuronic acid (GlcUA) and *N*-acetyl-β-D-glucosamine (GluNAc) alternately linked by (1→3) and (1→4) glycosidic bonds, respectively. Both residues exist in closed ring conformations, Figure 1.[4,7] The molecule is stabilized by intramolecular hydrogen bonds between the acetamido amide and carboxyl groups, across the β(1→4) linkage, as well as between the hydroxyl group and acetamido oxygen, across the β(1→3) linkages.[5] They give the polymer a two-fold helical structure in solution. There are two twists that total 360° bringing HA back to its original orientation. The G_1, N_1 disaccharide (Figure 1) is rotated 180° about the axis of the chain, compared with the disaccharide G_2, N_2. The radius of gyration is 200nm. The coil can be viewed as a highly hydrated sphere containing approximately 1000-fold more water than polymer.

The secondary structure of hyaluronan in aqueous solution proposed by Scott,[2] is based on electron microscopy with rotary shadowing technique. This showed that HA displays a network of aggregated chains. In aqueous solution, the secondary structure is stabilized by hydrogen bonds giving the polymer an expanded coil structure in solution. The

inner-residue, of the secondary structure, consists of a hydrophobic domain containing about 8CH units.[2] It is the hydrogen bonds, of the inner-residue, that contribute to the local conformational ordering.[3] The hydrophobic domains promote interpolymeric aggregation and form the basis of the formation of gels. Therefore HA has the properties of a highly soluble hydrophilic (water loving) material while also possessing properties of hydrophobicity (water hating), meaning, it is highly amphiphilic.[2] These chain-chain interactions of aqueous HA are of vital importance in the *in vivo* performances of biological fluids.[3]

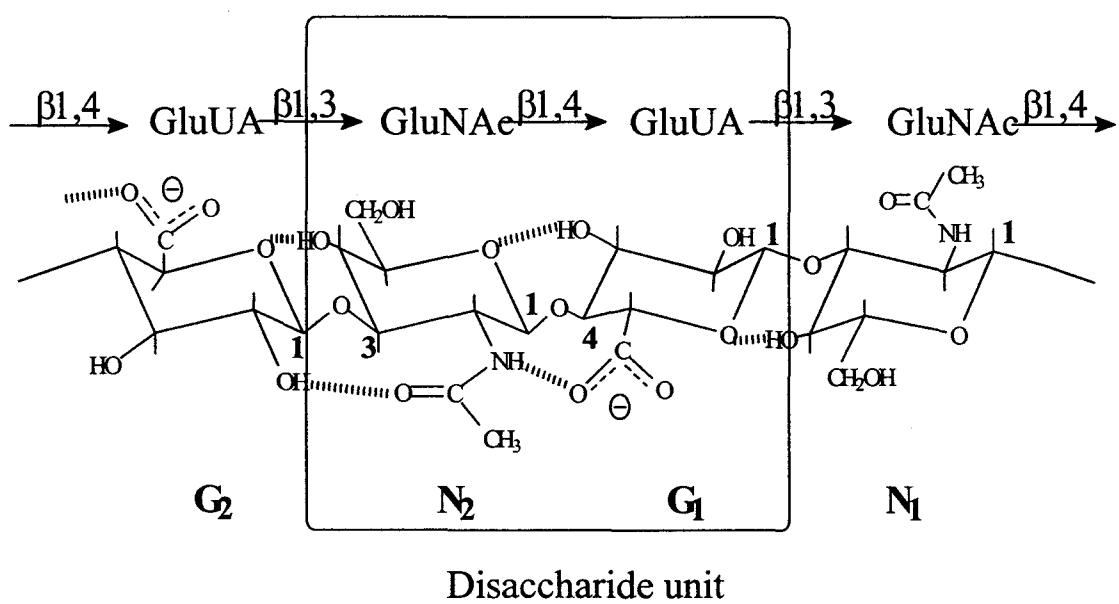

Figure 1. *Chemical Structure of hyaluronan. The polymer consists of alternating units of glucuronic acid (GluUA) and N-acetylglucosamine (GluNAc)*

1.1.2 Solution Properties of Hyaluronan

1.1.2.1 Polyelectrolytes in Solution

A polyelectrolyte is a macromolecule that has many ionizable groups. In aqueous solution polyelectrolytes dissociate into polyvalent macro-ions or polyions, and small counter ions of the opposite charge. It is the high charge of the macroion that produces a strong electric field which then attracts these counter ions. This attraction is the source of many of the characteristic properties of polyelectrolytes. In the presence of an increasing concentration of small ions (salt) the electrical effect of the polyion is screened.[8] Most polyions are long flexible chains that have a large extension in an aqueous solution. The size and shape will therefore depend on the charge and the interaction with the counter ions. As the charge increases, for an electrolytic macromolecule, the flexible chain will change its morphology from a contracted random coil to one that is fully extended. The relationship between the shape or the conformation and the electric state is another characteristic of polyelectrolytes.[8]

The interactions of the ionized groups and counter ions with water molecules, is greatly increased by the high charge density of the polyion. A small difference in the electrostatic interaction can have a great effect on the properties of the polyelectrolyte. Therefore, the polyelectrolyte is very sensitive to its structure and environment. The selective interaction of the counter ion with the polyion and the sensitive insolubilization of

the polyion by the specific counter ion are examples of this amplification.[8]

1.1.2.2 HA in Solution

Morris *et al.*[9] studied conformation and dynamic interactions of HA solutions. They reported the effects of changes in pH, salt, and temperature effects on the viscoelastic behavior of hyaluronan solutions. The techniques employed were viscosity measurements and small angle X-ray scattering.

Viscoelastic Behavior

Solutions of sodium hyaluronate at neutral pH and physiological ionic strength, show high viscosity, even at low concentrations, and display a gel-like character. This can be explained by the aggregation of HA with itself due in part to hydrophobic bonding between the hydrophobic patches.[2] Extensive investigations by viscosmetry[3] and light scattering measurements,[5,10] have shown that at neutral pH HA takes on the conformation of a random coil in solution.[9]

Influence of Acidic Conditions

Solutions of sodium hyaluronate were found to exhibit a reduction in viscosity at low pH, consistent with contraction of molecular coils upon protonation. On increasing the pH to neutral, the high viscosity can again be observed.[9]

Influence of Ionic Strength

An increase in the ionic strength in dilute solutions of HA at neutral pH, reduces the coil dimensions by screening the intermolecular charges. At high polymer concentrations, there is an increase in viscosity with increasing ionic strength due to the enhanced coupling of the polymeric chains while the intermolecular electrostatic repulsions are suppressed.[7,9]

Influence of Temperature

Hyaluronic acid solution viscosity under both neutral and acidic conditions has a discontinuity in its temperature dependence at 40°C. Instead of the linear Arrhenius behavior typical of a random coil the plots show a sharp discontinuity at this temperature, with a greater temperature dependence below this point than above. This indicates that the activation energy for network rearrangement at high temperatures is less than at low

temperatures.[3,9] Morris *et al.*[9] went on to explain that these results may be due to the melting out of intermolecular segmental interactions.

1.1.3 Interactions of HA and Surfactants

1.1.3.1 Polyelectrolytes and Oppositely Charged Surfactants

A general feature of systems that contain a polyelectrolyte and an oppositely charged surfactant is that under certain conditions phase separation takes place.[11] When charge neutralization is reached, i.e. when a surfactant is bound for each charged polyelectrolyte segment, phase separation can be expected.

The addition of an excess of salt can completely suppress phase separation. The concentration required to observe this phenomenon is called the critical electrolyte concentration, CEC. The concentration of salt required depends on the chain length of the surfactant as well as the concentration of the surfactant and the polyelectrolyte.[11]

When a surfactant of shorter hydrocarbon chain length is used there is a weaker attraction between the polyelectrolyte and the surfactant and also the formation of smaller micelles by the surfactant. The molecular weight of the polyelectrolyte is not very significant for this type of phase behavior.[11]

Bulk physical properties, such as viscosity, of mixed polymer/surfactant solutions are used to investigate the complexes that form, as well as the distribution of the surfactant

between the polymer, its free state, and aggregated state. Figure 2[12,13] provides a schematic representation of the interactions that occur between a polyelectrolyte and an oppositely charged surfactant.

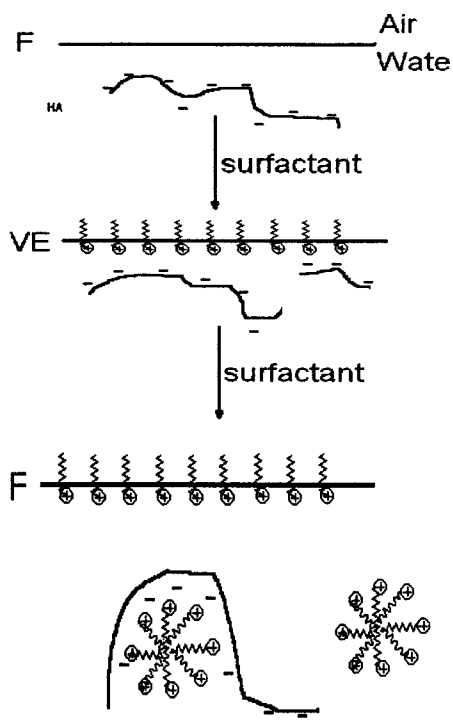

Figure 2. *Representation of the polyanionic HA and cationic surfactant interactions in the bulk and at the air/water interface. F, Fluid; VE, viscoelastic*[13]

1.1.3.2 HA and Oppositely Charged Surfactants

HA is a polyelectrolyte that has favorable electrostatic interaction with cationic surfactants. Surfactants bind to HA and influence both the conformation of the polymer chain and possibly its association with other HA molecules. Studies conducted by Fukada *et al.*[14] based on the interactions between HA and cetylpyridinium bromide, CTAB, in aqueous solution indicated that there was no difference in either the molecular size or the intermolecular interactions of the HA chains, compared to HA chains in NaCl solutions. Further investigation through the measurement of dynamic shear moduli by Fukada *et al.*[14] revealed that there is a small contribution by micelles to the rheology of the HA-CTAB system indicating that there is a loose and dynamic character to the surfactant binding to HA chains.[14]

Thalberg *et al.*[15] studied the interactions of HA with alkyltrimethylammonium bromides employing the techniques of phase separation, conductivity, NMR self-diffusion, and dye solubilization. They found that binding of surfactants to HA takes place only when the alkyl chain length is greater than 10 carbons. Also, due to the low linear charge density of HA the binding was found to be considerably weaker than with most other carboxylate polyelectrolytes. Through observations such as the high cooperativity and dependence on surfactant chain length, with regards to the counterion binding, and the solubilizing power of the surfactant bound to HA to a noncharged hydrophobic dye, it was determined that there

were micelle-like surfactant clusters adsorbed to the HA backbone. Thalberg *et al.*[15] also found that at a certain degree of binding, the HA-surfactant complex was no longer soluble and phase separation occurs. The two phase regions were found to extend to surfactant concentrations above the critical micellar concentration, CMC, and that further addition of additional surfactant would redissolve the precipitates. This was due to the electrostatic effects favoring the normal free micelles over the ones bound to the HA backbone. Therefore it was concluded that as the surfactant concentration was increased the surfactant ion activity decreased, leading to a decrease in the binding to the polyion.

1.2 Photochemistry and Photophysics

The way excited molecules can return to the ground state is by either a non-radiative or a radiative process, as represented in Figure 3. The Jablonski energy level diagram indicates the characteristics of molecular electronic states. In the singlet state (S_n, where n denotes the vibrational energy levels and is equal to 0, 1, 2, etc.) the electrons are spin-paired ($\uparrow\downarrow$) and the overall spin quantum number of the molecule is zero. The triplet excited state (T_1) has one of the electrons inverting its spin (spin forbidden by the selection rules of quantum chemistry) so that the two electrons are unpaired ($\uparrow\uparrow$), with the overall spin quantum number equal to one. At equilibrium, most molecules exist in the lowest energy vibrational level of the ground state (S_0). When the molecule absorbs a photon of light (hv)

from the visible or ultraviolet region of the spectrum electrons can be promoted to an excited electronic singlet state. When the excited molecule, from its singlet state, returns directly to the ground state, via a radiative transition, and emits a photon this is called fluorescence. Alternatively, the excited singlet state can undergo an intersystem crossing to an excited triplet state. A radiative transition from the excited triplet state to the ground singlet state is called phosphorescence.[16,17,18]

There are two ways to apply the technique of fluorescence spectroscopy when studying polymer solutions i) the use of a probe, where a fluorescent dye is merely dissolved in the polymer solution and ii) the use of a covalently attached dye. The latter will provide more information because the information obtained would be from the polymers perspective.[18]

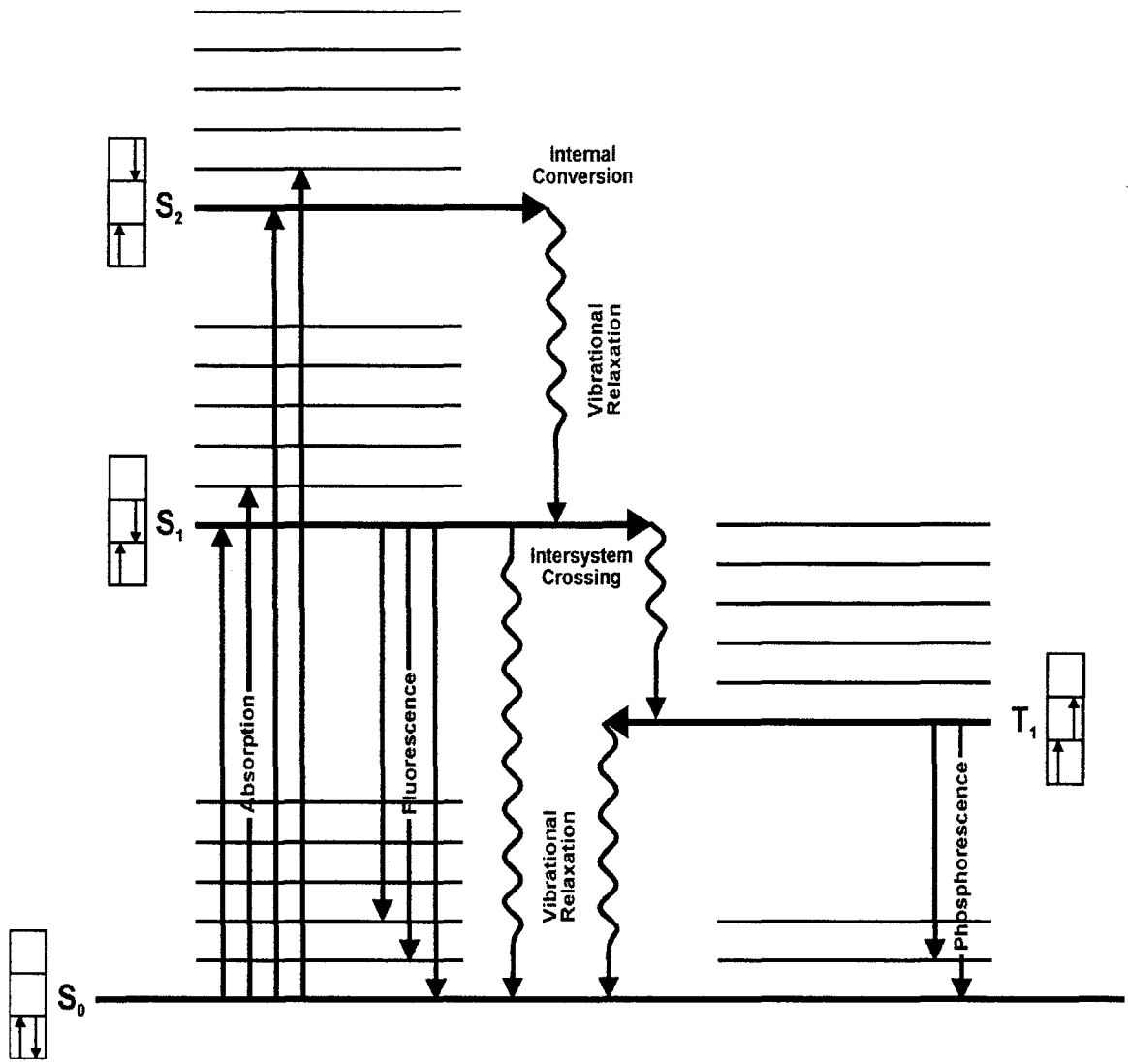

Figure 3. *Jablonski Diagram for a Typical Chromophore*

1.2.1 Fluorescence Lifetime

The fluorescence emission intensity of a chromophore exhibits a first order decay as shown in Equation 1:

$$I(t)=I_o e^{(-\frac{\tau}{\tau})} \qquad (1)$$

where τ is the time necessary for the fluorescent intensity to fall to 1/e of its initial value or the mean lifetime of the excited state. Relaxation that occurs only by fluorescence is termed the radiative lifetime, τ_F. Since the lifetime of the excited state depends on the rates of all of the relaxation mechanisms (Figure 3), as well as on the dissociation of the excited species into other products, this is seldom the case. The processes possible for relaxation of a molecule in the excited state, and their respective rate constants, are depicted below:

$^1M^* \rightarrow M + h\nu$	k_F (Fluorescence)
$^1M^* \rightarrow {}^3M^* \rightarrow M + h\nu$	k_{ISC} (Intersystem crossing and phosphorescence)
$^1M^* \rightarrow M$	k_{IC} (Internal conversion by vibrational relaxation)
$^1M^* \rightarrow$ **Products**	k_D (Dissociation into other products)

Since the last three mechanisms also contribute to the relaxation of the excited state, we can

write the observed fluorescence lifetime (τ_M) as:

$$\tau_M = (k_F + k_{ISC} + k_{IC} + k_D)^{-1} = (k_M)^{-1} \qquad (2)$$

where k_M is the total decay rate constant. For any given chromophore, the lifetime is sensitive to a variety of environmental factors including the concentration of the chromophore, matrix effects and the amount of impurities present. Measuring the fluorescence lifetime therefore can yield valuable information about the local environment of the chromophore.[19]

1.2.2 Fluorescence Quenching

Fluorescence quenching is the reduction of the fluorescence emission by a competing deactivating process, resulting from the specific interaction between an excited chromophore and another substance present in the system. Quenching has been divided into viscosity-dependent (dynamic) and viscosity-independent (static) types.[20]

All quenching mechanisms are considered bimolecular processes which are in competition with the emission, internal conversion, and intersystem crossing phenomena from the first excited singlet state of the chromophore. There are five types of quenching processes:

(i) Collisional quenching which is diffusion-controlled

(ii) Collisional quenching which is non-diffusion-controlled

(iii) Energy transfer quenching

(iv) Concentration quenching via excimer formation

(v) Radiative migration by self-absorption

Radiative migration is a property of the bulk solution and can therefore be examined by reducing the path lengths of the exciting and fluorescent light.

Concentration quenching is a useful indicator of the local chromophore concentration. This effect is a direct result of association of an excited fluorophore with a ground-state fluorophore producing an excited-state dimer or excimer which gives altered fluorescent properties:

$$^1M^* + M \rightleftarrows {}^1(MM)^* \qquad (3)$$

With diffusion and non-diffusion-controlled quenching, the process is described as complex formation, where this is a general term having no definite binding energy implied. Complex formation can occur either before or after excitation of ^1M to $^1M^*$;

$$
\begin{array}{ll}
{}^1M^* + Q \rightleftharpoons {}^1(MQ)^* & \\
\uparrow h\nu & (4) \\
M + Q \rightleftharpoons (MQ) &
\end{array}
$$

If the molar absorptivities of M and (MQ) at the exciting wavelength are ε and ε', then the fraction of incident light, α, absorbed by the complex ^{1}(MQ) is defined as,

$$\alpha = \frac{\varepsilon' K[Q]}{\varepsilon + \varepsilon' K[{}_1Q]} \qquad (5)$$

where K is the formation constant for (MQ) and is viscosity independent. If $k_{-Q} \rightarrow 0$ and (MQ) is nonfluorescent then,

$$\frac{\Phi_f{}^o}{\Phi_f} = (1 + kQ\tau_f[Q])(1 + K[Q]) \qquad (6)$$

where $\Phi_f{}^o$ is the unquenched quantum yield and Φ_f is the observed quantum yield for fluorescence of ^{1}M* in the presence of Q.

If the ground-state complex is negligible, then K ≈ 0 and Equation 6 becomes,

$$\frac{\Phi_f^o}{\Phi_f} = 1 + k_Q \tau_f [Q] \qquad (7)$$

The above equation is the classical Stern-Volmer equation for diffusion-controlled collisional quenching. The Stern-Volmer constant is given by,

$$K_{SV} = \frac{(\Phi_f^o / \Phi_f) - 1}{[Q]} = \tau_f k_Q \qquad (8)$$

If $k_Q = 0$, then the observed quenching is entirely due to ground-state complexation and Equation 7 becomes,

$$\frac{\Phi_f^o}{\Phi_f} = 1 + K[Q] \qquad K_{SV} = K \quad (9)$$

In both cases the observed quenching obeys a Stern-Volmer relationship.

When both processes are operating simultaneously, a plot of Φ_f^o/Φ_f versus [Q] will cease to be linear. Equation 9 predicts a linear increase in the Stern-Volmer quenching coefficient, K_{SV}, with increasing [Q]. The intercept and slope of a plot of K_{SV} versus [Q] will both increase with a decrease in solution viscosity and an increase in temperature.[21]

In the present study fluorescence quenching was one of the more valuable tools for

information about HA, with respect to structural effects. Four different quenchers were used, namely cetylpyridinium chloride (CPC), dodecylpyridinium chloride (DoPC), ethylpyridinium bromide (EtPy), and poly(N-ethyl-4-vinylpyridinium) bromide (VEP).

As shown in Section 1.2.2, fluorescence quenching can be described by the Stern-Volmer equation:

$$\frac{I_o}{I} = 1 + k_q \tau_o [Q] \qquad (10)$$

For these experiments, the fluorescent intensity of either DL or PMA was monitored as a function of the quencher concentration. For DL the intensity of fluorescence emission at 554 nm was chosen to represent the monomer intensity and for PMA the monomer peak was monitored at 376 nm. The fluorescence quenching of the dye-labeled HA samples with the pyridinium salts was expected to follow the Stern-Volmer model.

It is known that the pyridinium group is an efficient quencher of the singlet excited state of polycyclic aromatic hydrocarbons (PAH).[22-24] However, some alkyl pyridinium salts can act as surfactants capable of forming micelles in solution. The solubilization of a PAH into the micelle of a surfactant, such as CPC and DoPC, can cause two opposing effects; i) the stabilization of the singlet excited state of the hydrocarbon, with an increase in the fluorescence intensity, and ii) the quenching effect, which can cause either a partial or total inhibition of the fluorescence emission.[25]

Studies of quenching in the micellar medium when the surfactant acts as a quencher

were reported by Miola *et al.*.[26] They investigated the fluorescence quenching of amphiphilic derivatives of anthracene in the presence of micelles of N-cetylpyridinium bromide, chloride and nitrate. They showed that there was both static quenching of micelle incorporated probes, and dynamic quenching of the free probe in solution. Also, Sapre *et al.*[27] showed that the rate of fluorescence quenching of pyrene in the presence of CPC micelles below the CMC was diffusion-controlled, while above the CMC the quenching rate increased until it reached a point where it is independent of the surfactant concentration.

Whether a chromophore is covalently attached to a polymer or is simply present in solution, measurements of UV absorbance can be used to quantify the concentration of the chromophore. Also, quenching of a chromophore by a quenching species can be investigated for a system by UV spectroscopy. Time-dependent quenching in rigid micelles is normally described by Poisson quenching kinetics,

$$I(t) = I(0)e^{\left(\frac{-\tau}{\tau_o} - \frac{[\Theta]}{[\mu_1\chi]}(1 - \varepsilon^{-kt})\right.} \qquad (11)$$

where [mic] is the micelle concentration, [Q] is the quencher concentration, k is a pseudo-first order rate constant for the process and τ_0 is the lifetime of the chromophore in the micelles in the absence of quencher. Integrating this equation yields the time-independent form of the equation,

$$\ln\frac{I_0}{I} = \frac{[Q]}{[mic]} = \frac{[Q]N_{\alpha\gamma\gamma}}{[surf] - cmc} \qquad (12)$$

where I_0 and I are the intensities without quencher and at concentration [Q], respectively, [surf] is the surfactant concentration, and N_{agg} is the aggregation number of the chain ends.[16,19,28]

1.2.3 Luminescent Probes used in Determinating the Critical Micellar Concentration

Luminescence probes are utilized, in the determination of CMC's and CAC's, due to their sensitivity to their immediate environment (where the CMC is the critical micellar concentration and the CAC is the critical aggregation concentration).[29,30] An observation made by Hartley[31] in 1934 showed that the color of some dyes was modified upon adsorption in micelles.[29] Hartley also showed that the wavelength of maximum intensity of some dyes differed depending on the environment surrounding the dye. Based on the aforementioned results we have employed the use of PCA and DL to determine the CMC of CPC and DoPC. Some probes in a hydrophilic environment, such as water, will have a maximum intensity that differs from a hydrophobic environment. Using the difference in maximum intensities observed between a hydrophilic environment and a hydrophobic environment, one can determine the CMC or CAC by plotting the wavelength of maximum intensity versus the

concentration of surfactant.

1.3 Photophysics of Polymer Systems

1.3.1 Fluorescent Labels and Probes

Non-fluorescent polymers can be studied through photochemical techniques by using small fluorescent molecules or probes. An aqueous polymer solution that also contains a dissolved fluorescent dye is called a probed solution. This type of experiment is quantitatively useful if the dye binds to the backbone of the polymer. Another approach is to covalently attach a chromophore to the polymer backbone or to a sidechain. Valuable information can then be obtained on the physical properties of the polymer chains by investigating the interactions of these labels with themselves or with other species (e.g., excimer formation, quenching , etc.). An advantage to using labels is that they may be attached to the polymer in a variety of different ways. For example, labels may be attached randomly along a polymer backbone or just on the ends of the chain, depending on the properties one wishes to investigate. A probe, on the other hand, is a small fluorescent molecule that is mixed with a polymer in the solid state or in solution. The fluorescent properties of the probe depend on the polarity and steric restrictions of its environment, so that its migration through different regions can be observed. This technique will give information on such processes as phase separation and diffusion.[19]

The following probes were used:

1-Pyrenemethylamine (PMA) **1** has a very planar rigid structure.

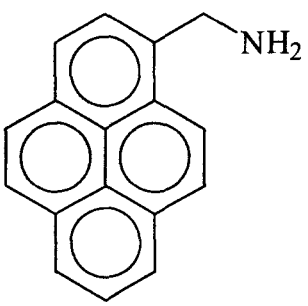

1

PMA has limited solubility in water and is considered hydrophobic. The fine structure of its fluorescence emission is between wavelengths 360-450 nm.

N-ε-Dansyl-L- Lysine Fluorescence

Dansyl lysine **2**, is a derivative of dansyl chloride which has the amino acid, lysine, in the N–ε position.

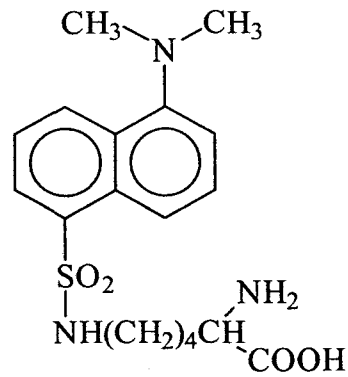

2

Studies conducted by Leezenberg *et al.*,[32] using dansyl lysine labeled polymer networks, revealed that the dansyl moiety showed a strong solvatochromic shift of its maximum fluorescence emission energy as a function of the polarity of its environment.[33]

Leezenberg *et al.*[32] indicated that the fluorescence signal from the dansyl in a multicomponent system can reflect the preferential solvation sensed by the molecule. The preferential solvation occurs because the fluorescent moiety itself locally perturbs its environment, whereby one of the molecules preferentially goes into the solvation shell of the probe.[32]

The solvatochromatic shift observed with the dansyl group can provide valuable information about the local environment of the probe. In an aqueous polymer solution it can yield information about the conformation of the polymer.

1-Pyrenylcarboxyaldehyde, **3**, (PCA) like PMA has a very rigid planar structure

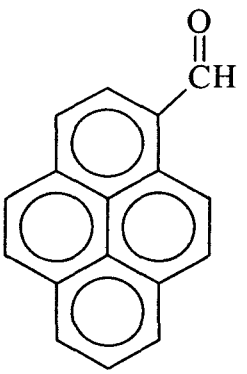

3

except that PCA like DL exhibits a dependence of the wavelength of maximum fluorescence emission intensity on the environment surrounding the dye. A blue shift is shown when PCA senses a more hydrophobic environment.[33] Therefore PCA, like DL, was used to determine the CMC of CPC and DoPC and the CAC of HA in the presence of the aforementioned surfactants.

Objectives

In trying to understand the function and behavior of hyaluronic acid (HA) in human tissue it is necessary to study the interaction of HA with other biological molecules, especially lipids, to predict the influence of HA will have on cell surfaces. We have chosen to investigate the interaction between HA and amphiphilic molecules (i.e., surfactants). Therefore, the objective of this study is to study the solution properties of HA using fluorescence spectroscopy.

2. Materials and Methods

2.1 Materials

Fluorescently Labeled Sodium Hyaluronate

Sodium hyaluronate was supplied by Hyal Pharmaceutical Corporation (Mississauga, ON) and was used without further purification. N-ε-Dansyl-L-Lysine (free acid) and 1-(1-Pyrenyl)-methyl amine, hydrochloride were purchased from Sigma and used without further purification. 1-Ethyl-3-(3-dimethylaminopropyl)carbodiimide, EDC, (99+%) and 1-Pyrenecarboxyaldehyde, PCA, (99%) were purchased from Aldrich Chemical Co. Cetylpyridinium Chloride, CPC, (99+%), Ethylpyridinium Bromide, EtPy, (98+%) Cetyltrimethylammonium chloride, CTAC, (98%), Tetradecyltrimethylammonium bromide, TTAB, (98%), and Dodecyltrimethylammonium chloride, DoTAC, (99%) were purchased from Sigma. CPC was recrystalized three times from methanol and EtPy was recrystalized from acetone. Dodecylpyridinium chloride was purchased from Tokyo Chemical Company and was used without further purification.

Poly(N-ethyl-4-vinylpyridinium) Bromide

Poly(4-vinyl pyridine) M.W. 1100 MWD 1.1 was purchased from Polymer Source Inc., and was used without further purification. Ethyl Bromide 98% and Propylene Carbonate, anhydrous, 99.7% were obtained from Aldrich Chemical Company.

Solvents

All solvents used were reagent grade. Methanol was obtained from Anachemia. Ethanol was obtained from Commercial Alcohol. Acetone, laboratory grade, was obtained from Caledon. Water was purified using a NANOpure deionizing system.

2.2 Instrumentation

^{13}C NMR spectra were recorded on Bruker AC200 and AC500 spectrometers. UV spectra were recorded on a Hewlett-Packard 8452 Photodiode Array spectrophotometer and operated through HP ChemStation Windows-based software. Dynamic light scattering data were acquired using a Brookhaven Instrument Corp. Model B19000AT correlator equipped with a Lexel Argon laser (λ = 514.5 nm) with the scattering angle set at 90°. The temperature was maintained at 298K and the refractive index and viscosity were set to

1.332Re, 0.8904, respectively. Data analysis was performed using CONTIN software provided by the manufacturer. Fluorescence spectra were recorded on a SPEX Fluorolog 212 spectrometer equipped with a DM3000F data system. Slit widths ranging from 0.5 to 4 mm were used depending on the chromophore concentration. The temperature of the water-jacketed cell holder was controlled by a Neslab circulating bath. The temperature of the sample fluid was measured with a thermocouple immersed in the sample. Emission spectra were recorded with an excitation wavelength of 328 nm for samples that contained dansyl lysine and at 340 nm for samples containing pyrenemethyl amine. Aqueous polymer samples were freeze-dried using a Benchtop 3L Virtis Sentry™ lyophilizer. Gel permeation chromatography (GPC) was performed using two ultrahydrogel columns (17.8 mm i.d., 30 cm length) equipped with a Waters 510 HPLC pump, Waters 410 differential refractometer, and a Waters 486 tunable absorbance detector (solvent was water, temperature was set to 30°C, and the flow rate was 0.7 ml/min). Calibration using standards for potentiometric measurements were made on a ORION model 290 A pH meter equipped with a DJ reference electrode using a Fisher Scientific bromide ion selective electrode model 13-620-520. All solutions were prepared with an ionic strength adjuster, ISA, 0.01M $NaNO_3$. Viscoelasticity measurements were performed using Petri dishes 10cm in diameter.[13,34] Ultrafiltration was done using an Amicon Ultrafiltration Cell Model 8200.

2.3 Methods

2.3.1 Pyrenemethyl amine Labeling

Hyaluronan sodium salt (HA) (200mg, 0.5 mmol disaccharide units) was dissolved in water (50 ml). 1-(1-Pyrenyl)methyl amine, hydrochloride (45 mg, 0.15 mmol) was dissolved in methanol (~3-5 ml) and added to this solution. The mixture was brought to pH 4.75 by the addition of dilute HCl (0.1 mol/L). To this solution EDC (384 mg, 2 mmol) was added and again the pH was adjusted to 4.75 using dilute HCl. The reaction was allowed to proceed at room temperature for 72 h. This mixture was then freeze dried. The freeze dried product was redissolved several times, in a minimum amount of water and precipitated into ethanol, to remove unreacted 1-(1-Pyrenyl)methyl amine and EDU (urea), the ethanol was removed via vacuum filtration, and then freeze dried, again. The amount of polymer isolated was 92.5 mg.

2.3.2 Dansyl Lysine Labeling

HA (1.0038 g, 2.5 mmol disaccharide units) was dissolved in 250 ml water to make a 4 mg/ml solution. N-ε-Dansyl-L-Lysine (22.07 mg, 0.058 mmol) was added to the solution in solid form. The resulting solution was brought to pH 4.75 by the addition of dilute HCl. To this solution EDC (373 mg, 2 mmol) was added and the pH was adjusted

again to 4.75 using dilute HCl. The reaction was allowed to proceed at room temperature for 24 h. The product was purified by ultrafiltration and precipitated several times, in an excess of ethanol to remove any unreacted dansyl lysine. The amount of polymer isolated was 500 mg.

2.3.3 Poly(N-ethyl-4-vinylpyridinium) bromide

Poly(4-vinyl pyridine) (193.27 mg) was dissolved in propylene carbonate (20 ml) containing absolute ethanol (1 ml). The solution was placed in an oil bath at 50°C under a nitrogen atmosphere. Ethyl bromide (95.6 mg, 5 mol excess to moles of poly(4-vinyl pyridine)) was added to the 50°C solution and the mixture was stirred for 24 hr and then cooled to room temperature. The polymer was isolated by precipitation into an excess of diethyl ether. It was filtered with a Millipore filtration apparatus using a type FH 0.5 μm teflon filter. The resulting polymer was extremely hygroscopic. It was isolated by freeze drying from water and kept under an inert environment (N_2). Poly(N-ethyl-4-vinylpyridinium) bromide was obtained in the amount of 66.58 mg.

2.3.4 The Talc Method for detecting Surface Viscoelasticity of HA[17]

Stock solutions of polymer were prepared by dissolving the polymer in water (1 g/L).

A stock surfactant solution in water was prepared at a concentration of 1 g/L. Mixed DTAB, TTAB, or HTAC/polymer solutions were prepared that spanned surfactant concentrations from 0.005 to 5.0 g/L. The surfactant/polymer solutions, at various concentrations, were mixed and allowed to stand in Petri dishes for approximately 30 min. A small quantity of calcinated talc powder was sprinkled on the aqueous surface, contained in a Petri dish. A gentle current of air was directed tangentially at the talc particles for a few seconds and then removed. The observed movement of the particles along the air/solution interface was recorded. The following qualitative characterizations of the interface were observed: F denotes a fluid interface; V, viscous; and VE, viscoelastic.[12]

2.3.5 Potentiometric Determination

Five standard solutions of potassium bromide were made from the dilution of a mother solution (0.13 mol/L). The concentrations and emf response were 6.6×10^{-5}M; 60.9 mV, 5.3×10^{-4}M; 11.0 mV, 8.4×10^{-3}M; -52.9 mV, 6.7×10^{-2}M; -100.9 mV and 1.3×10^{-1} M;115.7 mV. The potential (in mV) of each solution was measured using a bromide ion selective electrode coupled to a calomel double junction reference electrode, in 0.01 M $NaNO_3$. The potential of each solution was plotted versus concentration to provide a standard curve. The potential of the resulting polyvinylethylpyridinium bromide (-44.9 mV) was measured and this was used to calculate the degree of quaternization.

2.4 Characterization of Labeled Hyaluronate

2.4.1 Coupling Efficiency by UV analysis

The efficiency of the addition of the chromophore to the backbone of HA was determined by UV absorption analysis. A sample of the labeled polymer (5 mg) was dissolved in deionized water (50 ml). The absorbance of the solution was measured at 328 nm for dansyl lysine (DL) and at 340 nm for pyrenemethyl amine (PMA). Using Beer's Law the chromophore concentration was calculated. The extinction coefficient, ε, (38 224 cm L mol^{-1} for PMA and 24 777 cm L mol^{-1} for DL) was calculated from a solution of known concentration of chromophore. The ratio of apparent [DL] or [PMA] too expected [DL] or [PMA] provided an approximate coupling efficiency.

2.4.1.1 GPC analysis

A solid sample of the labeled polymer was dissolved in 0.1 M $NaNO_3$ and injected on to the column (1 g/L) to confirm the covalent attachment of the dye to the polymer. Wavelengths were monitored by the UV detector at 328nm for DL and 342nm for PMA. The temperature of the refractive index detector was set at 30°C. The flow rate was 0.7 ml/min.

2.4.1.2 NMR

^{1}H and ^{13}C NMR spectra were obtained on a Bruker AC500 NMR spectrometer for the unlabeled HA (10 mg), dissolved in D_2O (5 ml). Spectra were also taken for the labeled HA dissolved in D_2O to indicate if the chromophore was coupled to the polymer backbone.

2.4.2 Fluorescence Spectra of Labeled Polymers

Fluorescence spectra of aqueous solutions of labeled HA were taken as follows: DL labeled HA had an excitation wavelength set to 328 nm with emission being monitored from 450 nm to 610 nm. Slit widths were set at 2.0 to 4.0 mm, depending on the concentration of DL in solution. PMA labeled HA had an excitation wavelength set to 342 nm. The emission wavelength was monitored between 360 nm and 500 nm. Slit widths were set at 0.5 to 2.5 mm, depending on concentration. Data were acquired at 25°C.

2.4.3 Critical Micellar Concentration (CMC) Determination

The CMC of cetylpyridinium chloride and dodecylpyridinium chloride in water were measured by fluorescence,[35,36] using the chromophore dansyl lysine. The wavelength of the maximum intensity in the emission spectrum of dansyl lysine was plotted against surfactant concentration. The excitation wavelength was set to 328 nm. The inflection point of the resulting curve indicated the CMC of the surfactant.

2.4.4 Dynamic Light Scattering

Dynamic light scattering measurements of aqueous solutions of the labeled HA (1 g/L) in water were taken at 25°C as a function of VEP^+ to determine the approximate size of the complex formed.

3. Results and Discussion

3.1 Preparation and Characterization the Fluorescently Labeled HA used in this study

The same chemical reaction was used to attach the dansyl and the pyrenyl groups on the HA backbone,[37] as shown in Scheme 1 and Scheme 2. Before coupling, the carboxyl group of glucuronic acid on HA must be "activated". 1-Ethyl-3-(3-dimethylaminopropyl)carbodiimide hydrochloride salt, EDC, is used in the standard activation of carboxyl groups through formation of an activated ester, as shown in step 3 of the following reaction schemes. In step one HA and EDC are mixed in an aqueous solution and the pH is adjusted and maintained at 4.75. This pH is close to the pKa of the carboxylic acid group, of glucuronic acid, (on the HA backbone) and ensures the carboxylate form will be present. Also this pH assures the protonation of one of the nitrogens of the diimide of EDC providing a more electro positive carbon. Step 2 involves the nucleophilic attack by the carboxylic acid oxygen of the glucuronic acid on HA, to the electropositive carbon on EDC forming an activated ester. In step 3 the amide is formed by the nucleophilic substitution of the ester on the HA backbone with an amine, of the dye.

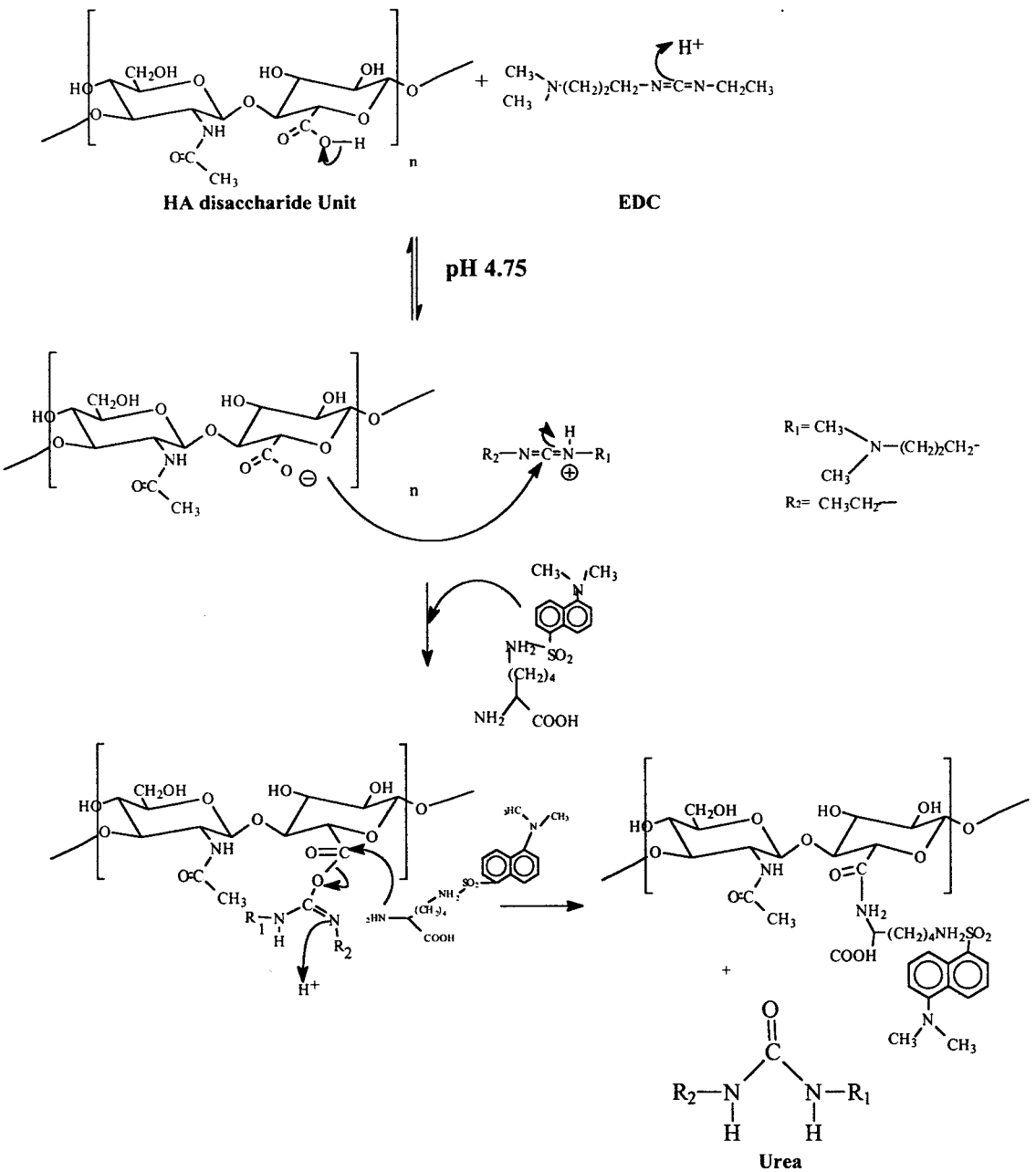

Scheme 1. *Synthetic scheme for the preparation of DL fluorescently-labeled hyaluronan*

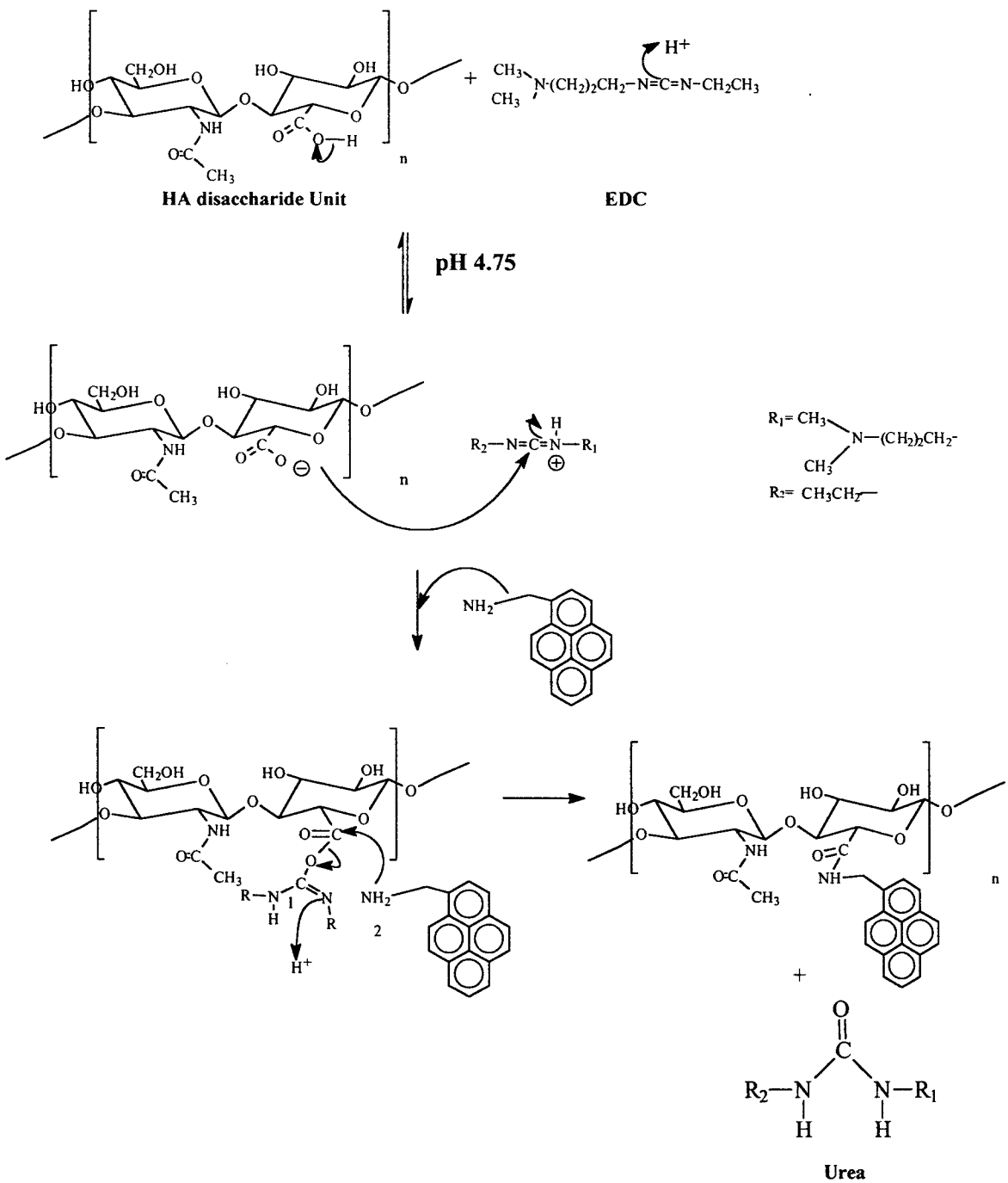

Scheme 2.*Synthetic scheme for the preparations of PMA fluorescently- labeled hyaluronan*

3.1.1 GPC

Gel permeation chromatography (GPC), based on size exclusion properties, is one technique used to obtain information about the covalent attachment of UV absorbing species, such as a dye, to the backbone of a polymer. In the presence of non-UV absorbing molecules such as carbohydrates, there will only be a single refractive index (RI) peak. Hence, the presence of UV absorbing molecules, such as dyes can be followed by UV. When a dye is covalently attached to a polymer that does not absorb UV light, overlapping bands will be shown on the RI and the UV traces. These overlapping bands indicate that the dye is covalently attached to the polymer.

With GPC, HA was injected initially to ensure the absence a low molecular weight UV-absorbing material. GPC of the unlabeled HA showed a single predominant band centered at 16.0 minutes, as seen in Figure 4.

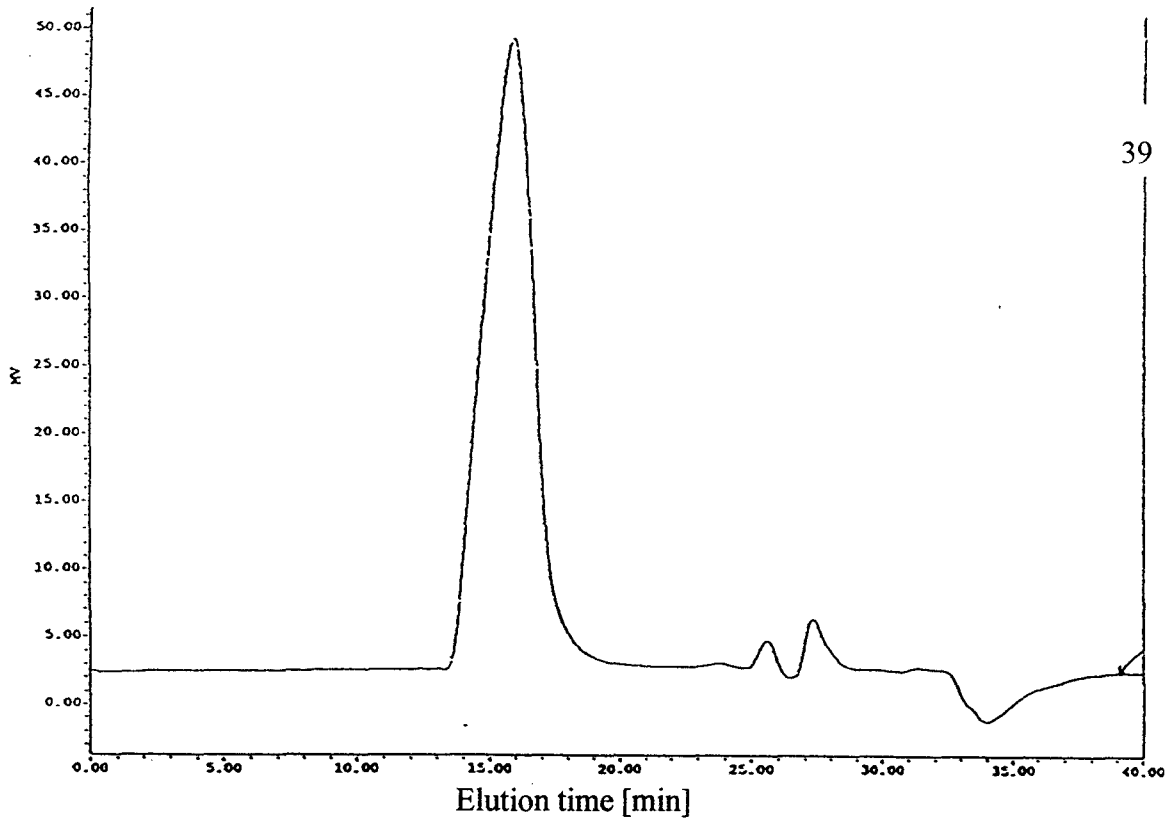

Figure 4. *GPC trace of HA (1 g/L) dissolved in 0.1 M $NaNO_3$. UV detector was set to 340 for PMA or 328 nm for DL. Temperature was 30°C*

The single band that appears in the trace of HA is produced by the refractive index (RI) detector. The corresponding UV trace (not shown) has no significant absorption, indicating the absence of UV absorbing species. Samples of labeled HA, on the other hand, produced strong UV and RI bands centered at 15.8 minutes for HA labeled with PMA, (Figure 5a) and at 15.7 minutes for HA labeled with DL, Figure 5b.

a)

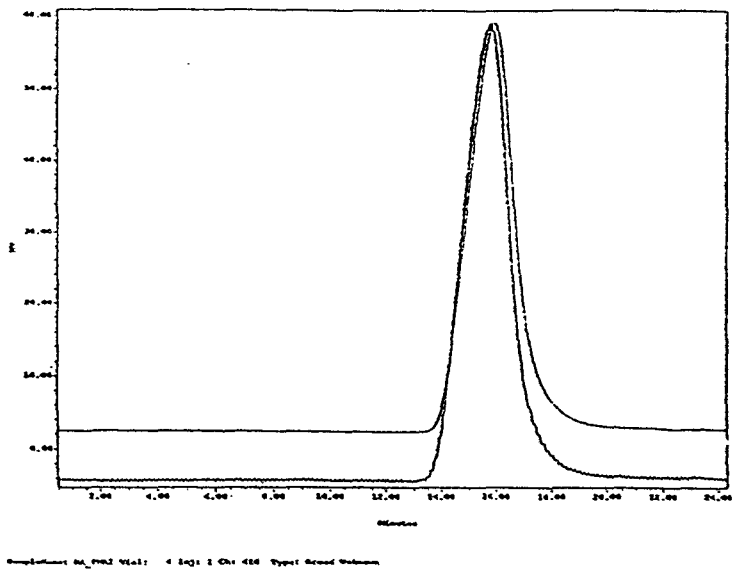

RI trace

UV trace

b)

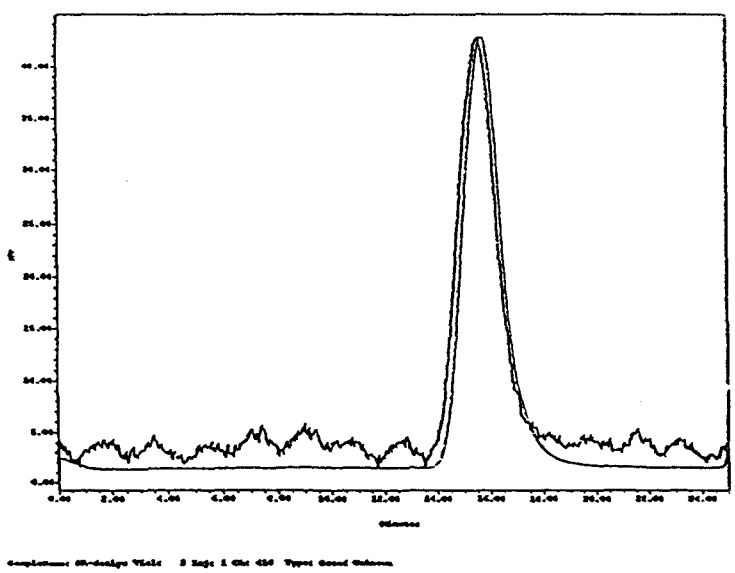

RI trace

UV trace

Figure 5. *GPC traces of labeled HA in 0.1 M $NaNO_3$. UV absorbance detector was set at a) 340 nm for PMA and b) 328 nm for DL. Temperature was 30°C*

Both GPC traces, Figure 5, show a UV absorption band which directly overlaps the RI band. The band produced by the UV detector is due to the presence of a UV absorbing species on the backbone of HA. This indicates that HA was successfully labeled.

3.1.2 UV Analysis

The efficiency of the chromophore coupling to HA, was quantified by UV measurements. The ratio of the apparent to expected concentrations of the dye gives an approximate coupling efficiency. The results are shown in Table 1.

Table 1: Amount of fluorescent label attached to HA

Fluorescent Label	*Mol % per HA Chain	Number of disaccharide units per label
Pyrenemethyl amine	0.73	121:1
Dansyl Lysine	4.3	21:1

$$*Mol\,\% = \frac{mol\ of\ label}{mol\ of\ disaccharide}\ X\ 100$$

Sample calculation:

$$\frac{1\ mol\ of\ dye}{121\ disaccharide\ units}\ X\ 100 = 0.73$$

3.1.3 Fluorescence Analysis

Fluorescence spectra of HA labeled with PMA and DL are shown in Figure 6.

a)

b)

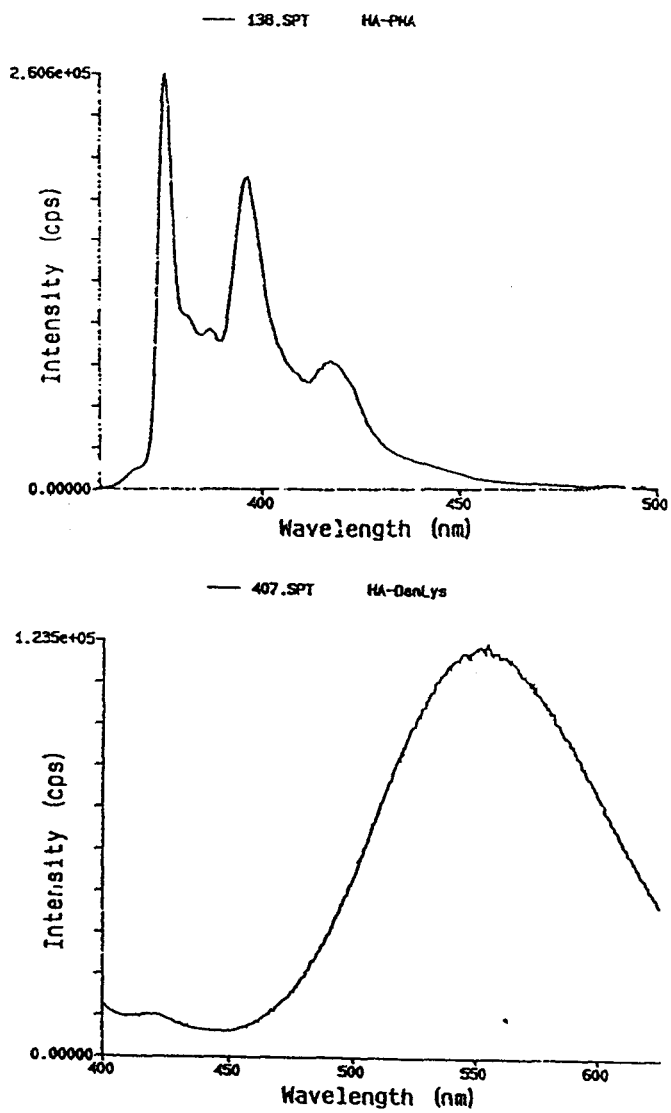

Figure 6. *Fluorescence emission spectra of labeled HA solutions in water: a) pyrenemethyl amine-HA (0.19 g/l, λ_{ex}:340 nm); b) Dansyl-HA (0.46 g/l, λ_{ex}:328 nm)*

Neither spectrum exhibits excimer emission, revealing the absence of inter- or intrapolymeric interactions between the labels.[35] The emission spectrum for the dansyl labeled HA shown in Figure 6b is weak, as is expected for the dansyl group in a hydrophilic environment.[38] The dansyl is almost insensitive to quenching by oxygen and trace amounts of impurities.[32,38] The emission quantum yield and the wavelength of maximum intensity however show a dependence on the polarity of the environment that surrounds the probe,[32] Section 1.3.1.

3.1.4 ^{13}C NMR Characterization

A literature review for the characterization of HA through NMR has revealed ^{13}C-NMR spectral data,[39] which were used to compare the ^{13}C NMR spectra obtained experimentally. ^{13}C NMR of HA was used to try and confirm the covalent attachment of the dye to HA, specifically the 5' carbon of glucuronic acid (see the scheme below).

^{13}C peak assignments:

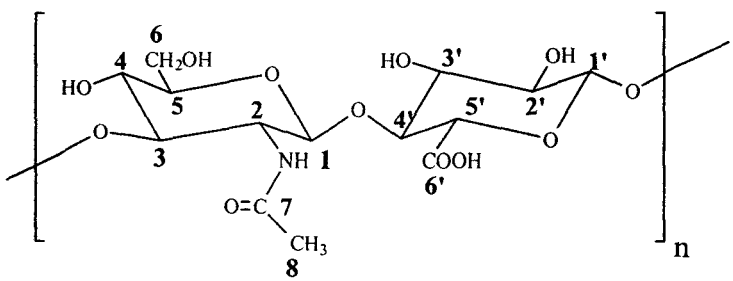

GluNAc **GluUA**

n = 1658

Table 2: ^{13}C NMR peak assignment for HA

Carbon #	Literature δ[39] (ppm)	Experimental δ (ppm)
1	103.11	103.25
2	56.98	54.59
3	85.20	82.85
4	71.06	68.54
5	78.07	
6	63.27	60.57
7	177.56	
8	25.18	22.53
1'	105.78	100.56
2'	75.20	73.63
3'	76.27	
4'	82.56	80.02
5'	78.90	76.13
6'	176.69	174.16

From the reaction scheme shown in Scheme 1, labeling of the dye to HA occurs at the carboxylic acid (**6'**) of glucuronic acid. However the chemical shift will not be seen because the carbonyl of amides require a bigger pulse delay in order to be observed. Carbon 5' would experience a change in chemical shift due to the covalent attachment of the dye. Spectral data, Appendix B, suggest that there may be a covalent attachment at this carbon however due to the low percentage of label on HA (DL 4.3% and PMA 0.73%) no definitive information could be concluded. The high viscosity of HA solutions (> 1 g/L) did not allow for an increase in concentration to detect the covalent attachment of the dye.

3.2 Preparation of Poly(N-ethyl-4-vinylpyridinium) Bromide

Poly-4-vinylpyridine[40] was modified with ethyl bromide to give poly(N-ethyl-4-vinylpyridinium) bromide (VEP), as described by Eisenberg *et al.*.[41,42,43] The synthetic scheme is shown in Scheme 3,

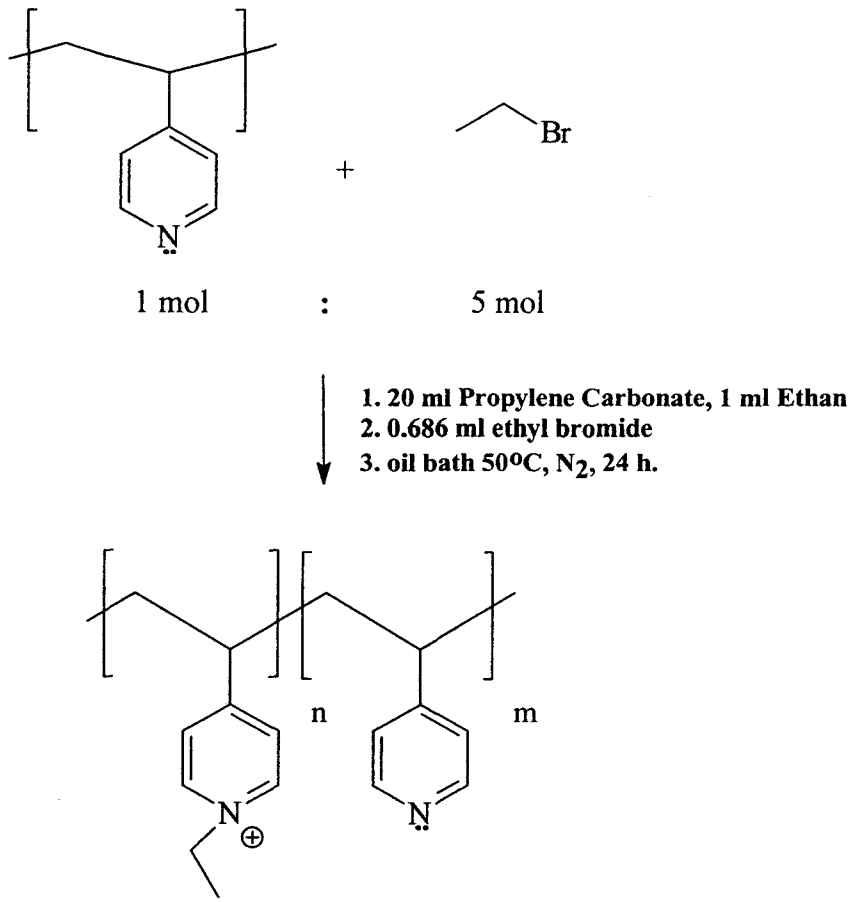

poly(N-ethyl-4-vinylpyridinium) bromide

Scheme 3. *Synthetic scheme of poly(N-ethyl-4-vinylpyridinium) bromide: n = 7; m = 3*

The degree of quaternization of pyridine was determined by measurement of the bromide concentration using an ion selective electrode. The electrode was calibrated against the potential from bromide solutions of known concentration, as shown in Figure 7. VEP was found to contain 7 bromide ions per chain.[44] The potential was plotted as a function of

bromide concentration and an equation is generated for the resulting curve. The potential is then measured of a aqueous solution of polyvinylethylpyridinium bromide, of known concentration, enabling calculation, from the resulting curve, of the percentage of bromide ions in the VEP^+ solution.

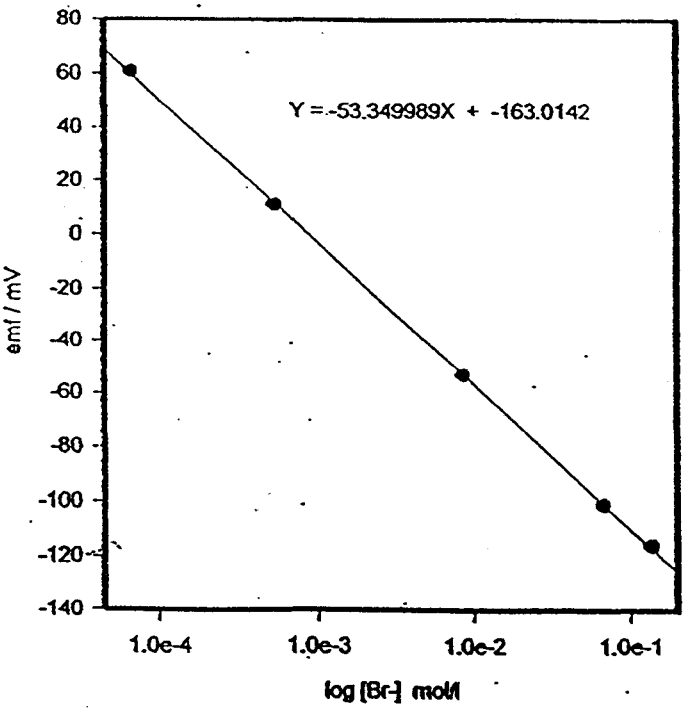

Figure 7. *Calibration curve used for determining the number of bromide ions per poly(N-ethyl-4-vinylpyridinium) bromide chain*

3.3 Interactions of HA and VEP

Dynamic light scattering measurements of HA as a function of VEP concentration were performed to see if there were polymer/polymer interactions and the size of the aggregates that formed. This was based on the phase separation observed when HA was mixed with VEP. The following results were obtained:

Table 3: Dynamic light scattering of HA/VEP interaction @298K. Concentration of HA in solution was 1 g/L = 2.1 X 10^{-3} mol of disaccharide/L

Concentration of VEP	Size of HA/VEP aggregates
1.701 X 10^{-4} M	280 nm
2.721 X 10^{-4} M	860 nm
3.400 X 10^{-4} M	1525 nm
5.182 X 10^{-4} M	2180 nm

The dynamic light scattering experiments were performed first on solutions of either HA or VEP. No signal was detected since there is no interpolymeric aggregation in this case. However, the mixed solution of HA and VEP, Figure 8, show a linear relationship between the size of aggregates formed and the concentration of VEP present in the system. Light scattering measurements conducted by Sheehan *et al.*[10] using mono and divalent cations namely sodium, potassium and calcium interactions with hyaluronate chains showed that

there was a significant increase in HA segmental interactions in the presence of these cations, especially in the presence of Ca^{2+}.[45] These results are similar to the ones obtained here with the exception that here it is polyelectrolyte/polyeletrolyte interactions.

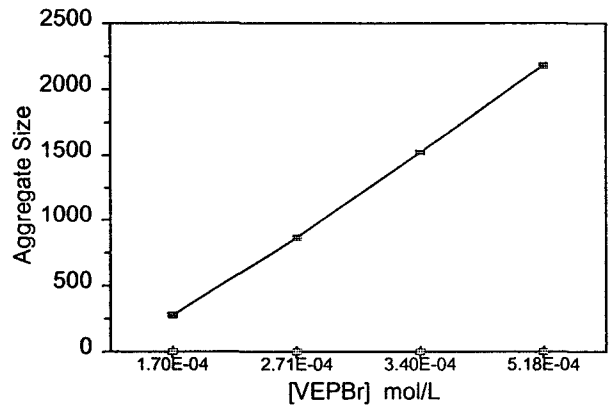

Figure 8. *Increase in the aggregate size of HA VEP as the [VEP] is increased*

The increase in the aggregates observed with HA and VEP is due to the presence of the pyridinium groups of the VEP, shielding the anionic charge of HA and allowing interaction of VEP molecules.[10,46,47]

3.4 Polymer-Surfactant Interactions

Surfactant molecules interact with polymers at a critical aggregation concentration (CAC), forming micellar-like aggregates along the polymer chain. The CAC is generally lower than the critical micellar concentration (CMC) of the surfactant in a polymer-free solution. The polymer will become saturated with surfactant molecules, and then free micelles will appear. This association is dependent on both the relative charge and the hydophobicity of the polymer-surfactant pair. In the case of charged polymers and oppositely charged surfactants there is the formation of salt bonds between the polyelectrolyte monomeric units and the surfactant head group.[13]

To enable the photochemical study of polymer-surfactant interactions one adds to the system a luminescent dye which is free to diffuse in solution (termed "probe") or attached via a covalent bond to the polymer (termed "label"). Fluorescent probes can be used in the determination of (1) the CAC of the polymer-surfactant pair; (2) the aggregation number of the polymer-surfactant association and (3) the microenvironment sensed by the probe within the matrix of the complex.[13]

Three types of measurements were performed in aqueous solution:

(1) probe plus surfactant (CMC determination)

(2) HA-label plus surfactant

(3) HA plus probe plus surfactant

3.4.1 CMC determination of CPC and DoPC

Surfactant solutions spanned the concentration range of 10^{-6} to 10^{-1} M. The concentration of HA was kept constant (~ 1g/L). The surfactant concentration range was chosen to ensure that it included the reported CMC of the surfactant, (CMC for CPC[46] of 9 X 10^{-4} M and for DoPC[49] of 1.5 X 10^{-2} M). The wavelengths of maximum fluorescence intensity over these concentration ranges were measured for DL (ca. 3.83 X 10^{-3} M) and PCA (ca. 2.5 X 10^{-6} M) in aqueous solutions, see Figure 9. As the probe is solubilized into the hydrophobic environment of the surfactant micelle, there is a shift in the wavelength of maximum emission observed. This wavelength shift is plotted as a function of surfactant concentration to determine the CMC.[50]

a)

b)

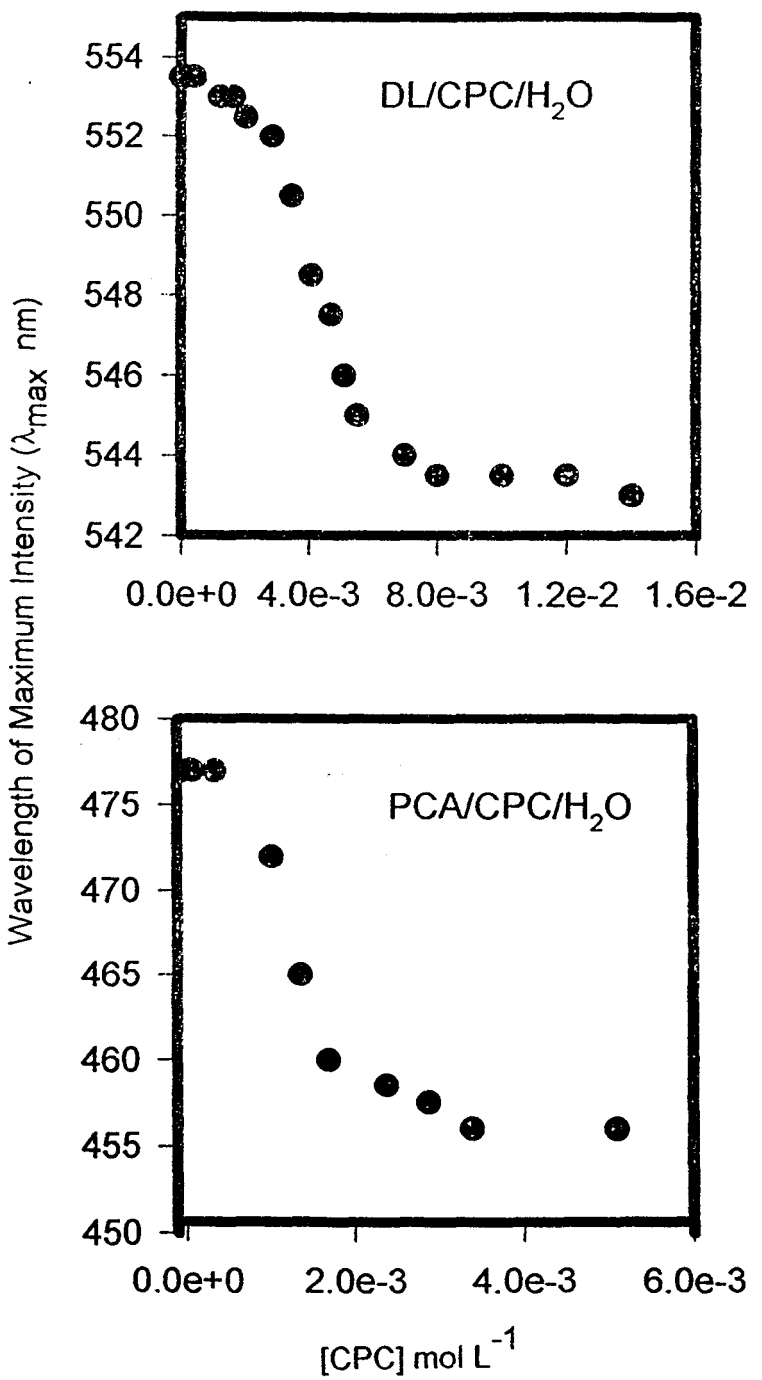

Figure 9. *Dependence of the wavelength of maximum intensity on surfactant concentration for CMC determination: a) DL λ_{ex} = 328 nm; b) PCA λ_{ex} = 363 nm*

The change in the emission wavelength maximum is 477-455 nm for PCA, Figure 9b, and 553-542 nm for DL, Figure 9a. The inflection point of the curve indicates the CMC for the surfactant. CMC values are shown in Table 4.

3.4.2 Determination of the CAC of various Surfactants in the Presence of HA: Probe Studies

The change in wavelength of maximum intensity were measured for HA with either DL (450-620 nm) or PCA (350-550 nm) in aqueous solutions containing a fixed amount of polymer (~ 1 g/L) and increasing amounts of CPC or DoPC, seen in Figure 10. The concentration ranges used for CPC and DoPC were limited by phase separation, see Section 1.1.3.1. Solubilization of the DL or PCA probe into a hydrophobic environment, as detected by the blue shift in the wavelength of maximum intensity for both DL and PCA, was observed for CPC and DoPC at concentrations higher than 6.8×10^{-5} mol L^{-1} for CPC, and 1.02×10^{-4} mol L^{-1} for DoPC. With increasing CPC or DoPC concentration, the blue shift observed increases until a saturation value was reached of ~1.36×10^{-3} mol L^{-1}, for CPC, and ~8.12×10^{-4} mol L^{-1}, for DoPC, a concentration which is lower than the CMC of either CPC (9×10^{-4} mol L^{-1})[48] or DoPC (1.5×10^{-2} mol L^{-1}).[49] The blue shift observed with both the DL and PCA occurs over a large surfactant concentration range as opposed to a sharp transition which is centered about the critical micellar concentration, this behavior is observed more commonly with neutral polymers such as PEO,[50] and/or PVP.[50]

a)

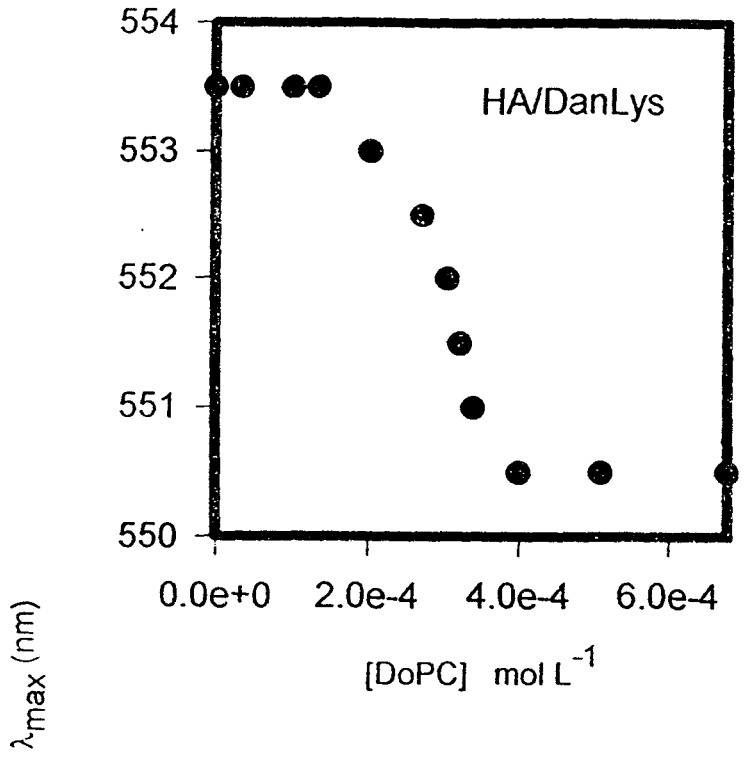

b)

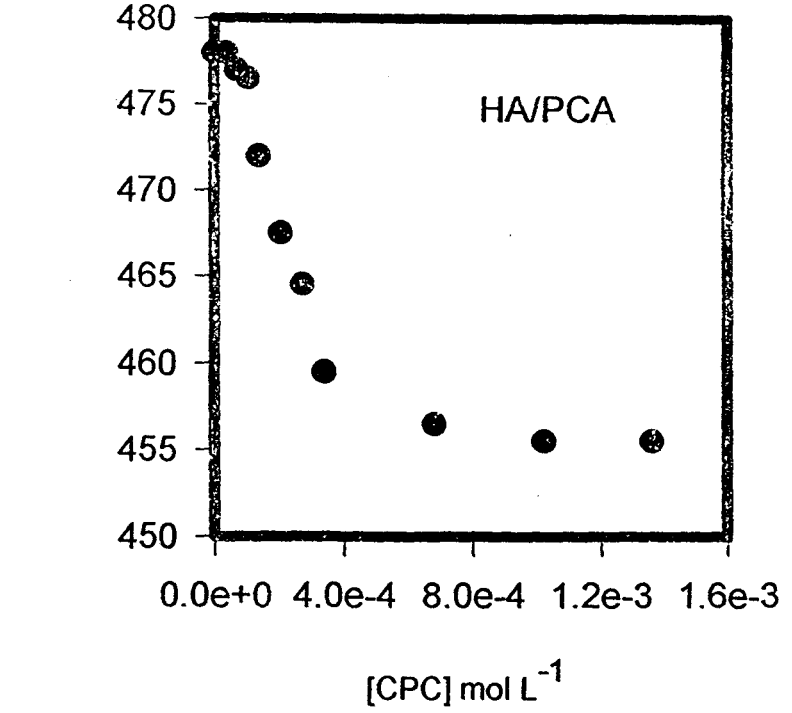

Figure 10. *Plot of the shift in the wavelength of maximum intensity, for the emission of DL and PCA in aqueous solution of HA (1 g/l) as a function of surfactant concentration (logarithmic scale) for CPC and DoPC. T=25oC;* λ_{ex} *= 328 and 363 nm for DL and PCA respectively*

The spectroscopic data lead to the following description of the interactions of surfactants with polyanionic HA, Figure 11. HA is known to adopt a worm like conformation in solution.[46] The addition of minute amounts of cationic surfactant will disrupt the HA network by the adsorption of the hydrophobic tail on the polymer backbone, as well as electrostatic attraction between poly anionic HA and the cationic head group, of the surfactant molecule. The addition of more surfactant results in the formation of surfactant aggregates on the HA backbone, until a limiting point is reached where free surfactant micelles are formed in solution.[15,51,52]

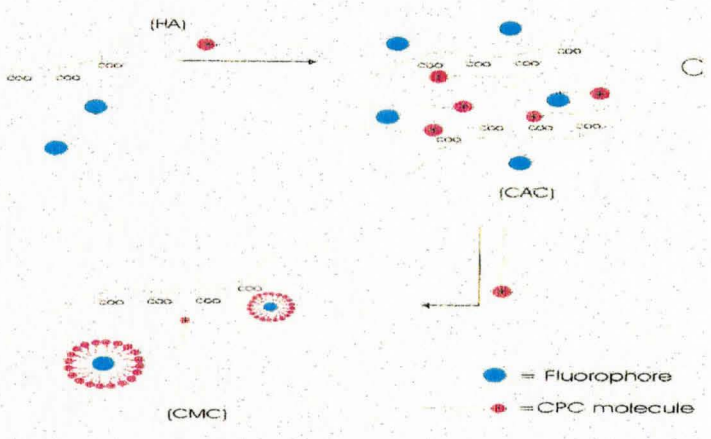

Figure 11. *Schematic representation of the interactions between probed HA solutions and CPC or DoPC*

3.4.3 Determination of the CAC of various Surfactants in the Presence of labeled HA

The covalent attachment of a label to HA enables one to monitor the mechanism of adsorption of a surfactant micelle, to the polymer chain. This is accomplished by the incorporation of the label into the hydrophobic core of the micelle. The CAC of labeled HA with either DL or PMA were determined in the same way as those of probed solutions of HA (Section 3.3.2). The results of the CAC and CMC determinations are shown in Table 4.

Table 4. Critical aggregation concentration (CAC) and critical micellar concentration (CMC) values for CPC (CMC 9 X 10^{-4}M) and DoPC (CMC 1.5 X 10^{-2}M) in aqueous solution of aqueous dye, HA/probe or HA-dye.

	CPC		DoPC	
Dye Used	**CMC (mol/L)**	**CAC (mol/L)**	**CMC (mol/L)**	**CAC (mol/L)**
PCA	1.23 X 10^{-3}	-------	1.77 X 10^{-2}	-------
DL	1.02 X 10^{-3}	-------	1.24 X 10^{-2}	-------
HA/PCA	-------	1.47 X 10^{-4}	-------	1.94 X 10^{-3}
HA/DL	-------	2.99 X 10^{-4}	-------	8.76 X 10^{-3}
HA-DL	-------	1.43 X 10^{-4}	-------	4.91 X 10^{-3}

3.5 Fluorescence Quenching Experiments

The quenching studies were done to establish the differences that exist in the quenching processes taking place with DL and PMA. Different solutions were used that contained CPC, DoPC, in the form of monomer, premicellar aggregates, or micelles.

The quenchers, CPC, DoPC, EtPyBr and VEPBr were employed for fluorescence quenching experiments. These compounds all contain a pyridinium moiety which is a quencher of pyrene fluorescence, but they also differ in solubility and hydrophobicity. The pyridinium quenchers CPC and DoPC are surfactants differing by two carbon units, EtPyBr is not considered a surfactant because it contains an allylic chain of two carbon units. As the alkyl chain length increases the solubility decreases therefore, EtPyBr is more soluble than CPC. These quenchers are considered small molecules. To study quenching as well as polymer-polymer interactions[53,54,55] VEPBr was used, where VEPBr contains seven pyridinium moieties, see Section 3.2, and is considered a small polymer. To study the quenching effect of a non-surfactant EtPyBr was used.

In the cases of the aqueous solutions of either HA mixed with DL or PMA, or HA labeled with DL or PMA the concentrations of CPC, DoPC and VEPBr used were limited, due to phase separation. These areas of phase separation are indicated on the Stern-Volmer plots by dotted lines. As the binding ratio reaches one surfactant ion per charged HA disaccharide unit, this phase separation is expected.[11]

3.5.1 Quenching studies of Aqueous solutions of DL and PMA

The Stern-Volmer plots for the fluorescence quenching of DL (ca. 2.69 X 10^{-4} mol L^{-1}) and PMA (1 X 10^{-6} M) in aqueous solution, upon addition of CPC, DoPC, EtPy and VEP are shown in Figure 12. The linearity of these curves indicates that the quenching mechanism obeys the Stern-Volmer model. The linear regression lines are also included on the graph. In all cases the slope of the lines equal to the Stern-Volmer quenching constant, K_{SV}, for DoPC, EtPy, and VEP is lower than in the case of CPC, see Table 5. The large K_{sv} suggests the observed quenching is due to static quenching.[25]

Table 5. Stern-Volmer constants, K_{SV}, for various pyridinium salts.

K_{SV} (M^{-1})

	CPC	DoPC	EtPyBr	VEP
PMA	780	730	690	32
DL	440	72	31	19
HA/PMA	3400*	510*	490	24*
HA/DL	170*	110*	23	16*
HA-PMA	40*	390*	500	15*
HA-DL	340*	46*	18	8*

* final slope of upward curvature (see text)

a)

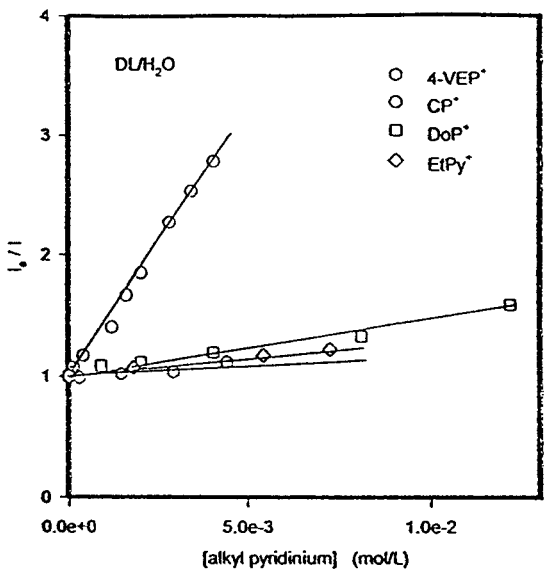

b)

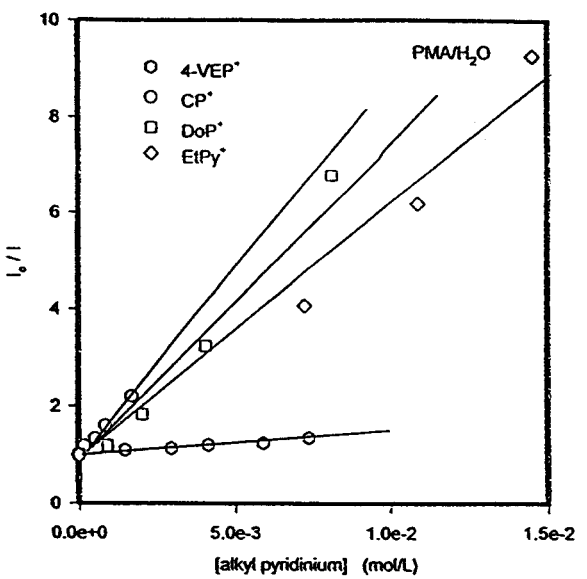

Figure 12. *Stern-Volmer plots for Pyridinium salts quenching of aqueous DL and PMA @298K; a) DL* λ_{ex} *= 328 nm and b) PMA* λ_{ex} *= 342 nm*

3.5.2 Quenching Studies of HA probed and HA Labeled with DL or PMA

Quenching studies of probed solutions of HA are shown in Figure 13. Quencher concentrations ranged from 2 X 10^{-4} M - 7 X 10^{-4} M for CPC, 1 X 10^{-4} M - 4 X 10^{-3} M for DoPC, 2 X 10^{-5} M - 1 X 10^{-2} M for VEPBr, and 9 X 10^{-3} M - 9 X 10^{-2} M for EtPyBr see Figure 13. Studies of labeled HA with DL (0.338 g/L) and PMA (0.19 g/L) were also performed in the same aforementioned concentration range of CPC, DoPC, EtPy, and VEP are shown in Figure 15. The cationic quencher molecule causes a decrease in the anionic repulsions between HA chains thus enabling HA chains to come into closer contact, see Section 3.2.2. A control experiment with potassium bromide was performed to see if the fluorescence quenching could be partly attributed to the presence of the bromide ion (see Figure 13) as halogens are known fluorescence quenchers.[56] There was little to no difference in the emission spectra of aqueous solutions of DL, PMA, HA/DL, HA/PMA, HA-DL or HA-PMA, as a function of bromide concentration. This indicates that the emission quenching was most likely due to the presence of the pyridinium ion.[25]

The quenching results for the solutions of HA probed with DL (ca. 3.33 X 10^{-5} M) and PMA (ca. 1 X 10^{-6} M) are shown in Figure 14. Straight lines were obtained for CPC below 2 X10^{-4} M, DoPC below 5 X10^{-4} M, and VEP below 1 X 10^{-4} M. The fluorescence quenching of DL and PMA, in the presence of HA, must be due to static or dynamic quenching processes. However, above a concentration of 10^{-4} M for CPC, DoPC, and

VEPBr there was deviation of linearity in the respective Stern-Volmer plots. These deviations were positive (curvature toward the y-axis). They may result from a combination of dynamic and static quenching mechanisms, Figure 16. The large K_{SV} for CPC (3.4 X 10^3 M^{-1}) in probed solutions of HA/PMA is primarily due to static quenching, considering that quenching requires close contact between the fluorophore and the quencher.[18]

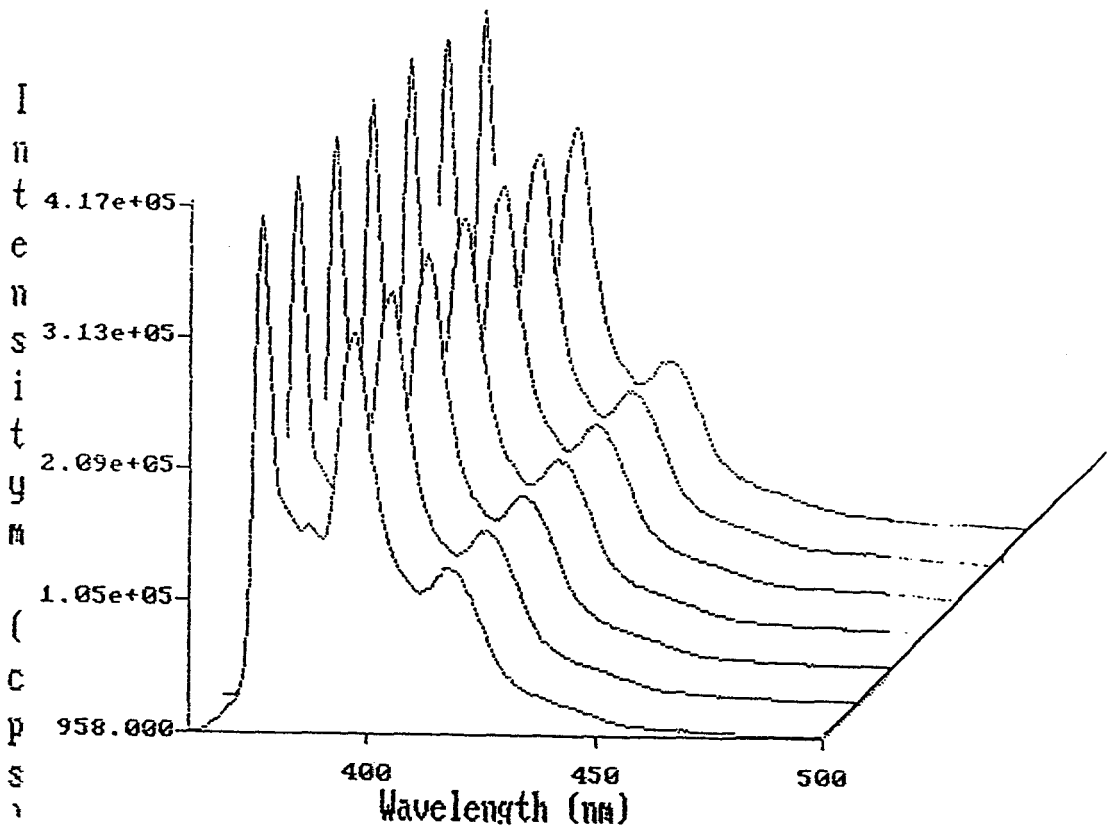

Figure 13. *Plot of fluorescence emission spectra of HA labeled with PMA as a function of bromide concentration,* λ_{ex} *= 342 nm;* λ_{em} *= 350 - 500 nm*

a)

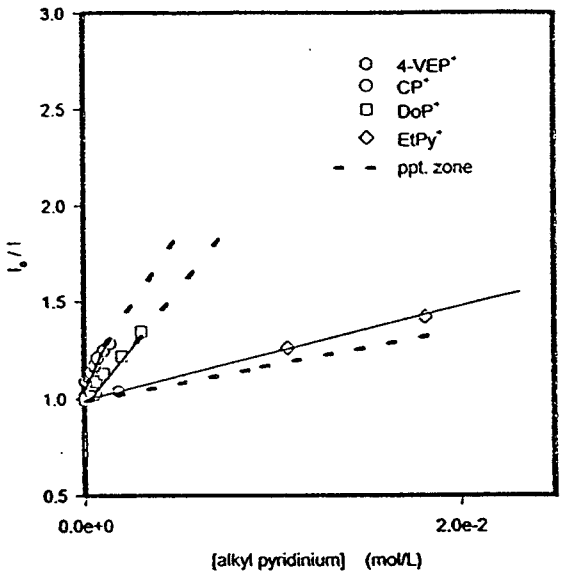

b)

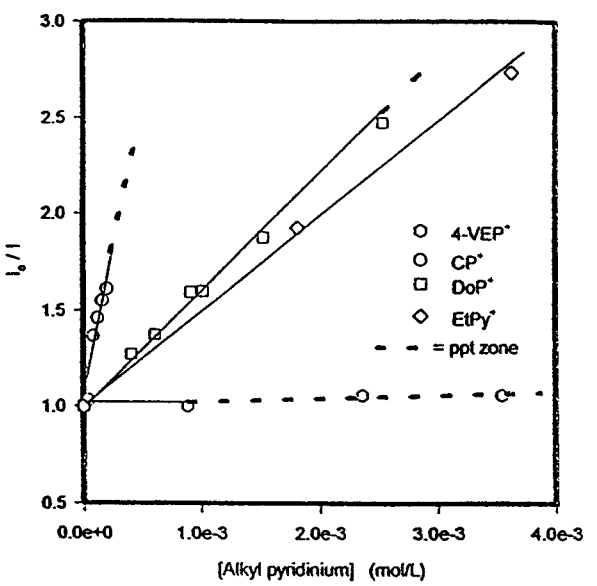

Figure 14. *Stern-Volmer plots of probed solutions of HA (1 g/L) with a) DL (3.33 X 10^{-5} M) λ_{ex} = 328 nm, and b) PMA (1 X 10^{-6} M) λ_{ex} = 342 nm*

a)

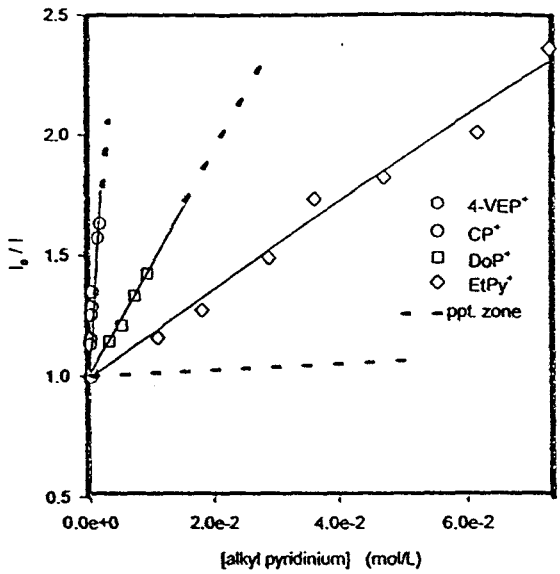

b)

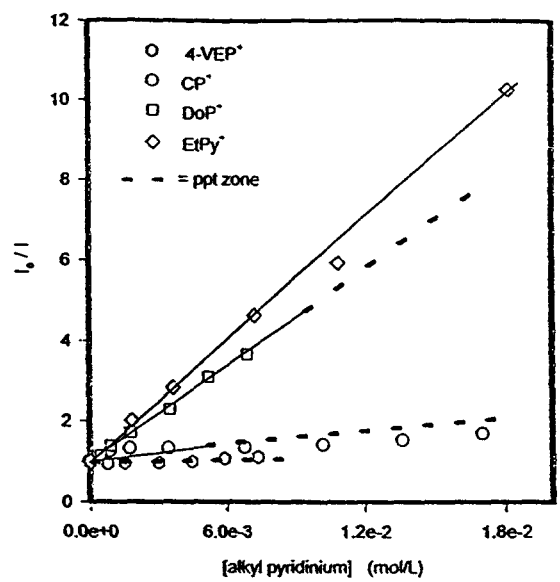

Figure 15. *Stern-Volmer plots for labeled solutions of HA with a) DL λ_{ex} = 328 nm (0.338 g/L), and b) PMA λ_{ex} = 342 nm (0.190 g/L)*

Dynamic quenching is directly related to the nonradiative deactivation of the fluorophore molecules in the excited state, by collisions, fundamentally, with a quencher molecule. Conversely, static quenching is a very rapid process, which may cause a decrease in the fraction of excited fluorophore molecules before they are dynamically quenched.[57] As a result, the Io/I relationship can increase much faster than expected on the basis of the aforementioned mechanisms, because both are directly related to the concentration of the quencher molecules. Therefore, a combination of static and dynamic quenching mechanisms can cause an upward curvature as observed in this case for both DL and PMA in aqueous solutions of HA.[25] This loss of linearity of the Stern-Volmer equation occurs because only a part of the dye hydrocarbon molecules are deactivated by collisional mechanisms, while the rest form a complex in the ground state.[57,58]

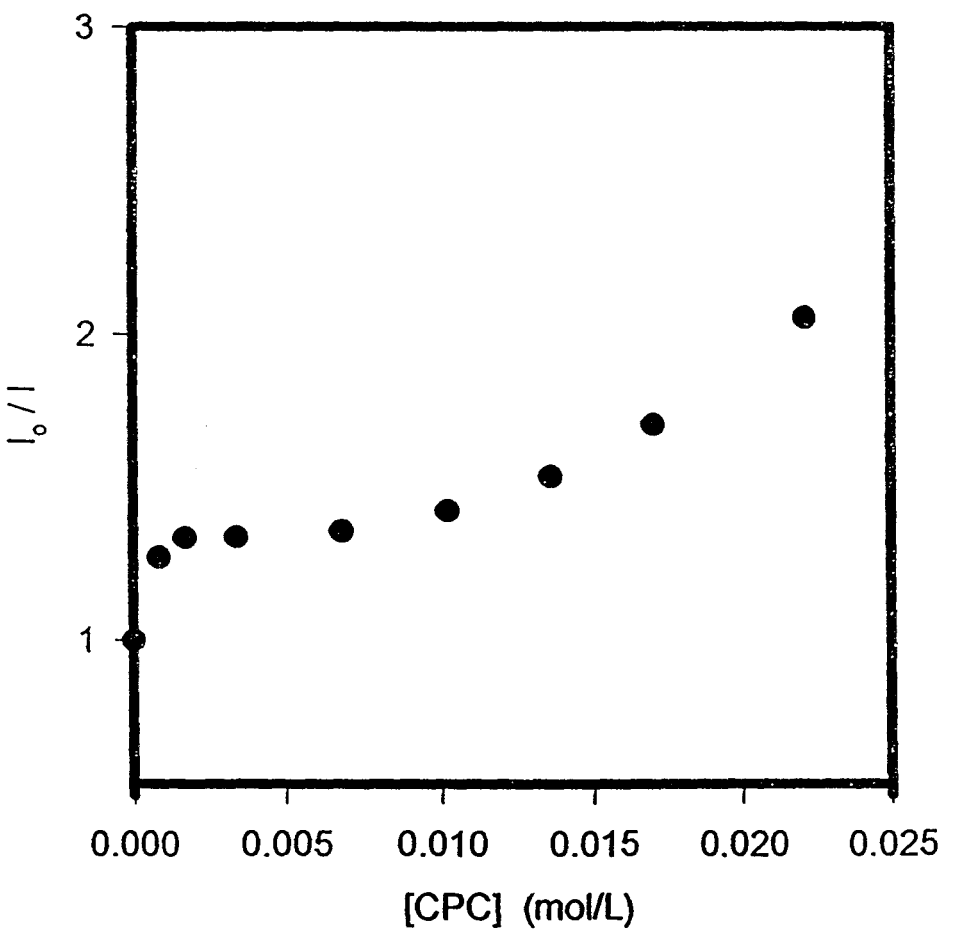

Figure 16. *Deviations of the Stern-Volmer equation.*

3.6 HA Surface Properties (The Talc Test)

HA is known to interact strongly with cationic surfactants.[15] Phase maps representing the dilute aqueous mixtures of HA/alkyltrimethylammonium halides are shown in Figure 17. It is apparent, from Figure 17, that there is surface viscoelasticity over a large range of surfactant concentration for HTAC and TTAB, but this is not shown for DTAB. For the system containing DTAB, the surface remained viscous at low surfactant concentrations and became fluid at surfactant concentrations greater than 1.0 g/L. The HTAC/ HA and TTAB/HA solutions that show viscoelasticity contain relatively low concentrations of surfactant. When fluidity is shown to be present in the system, it is due to the formation of polymer/surfactant aggregates or the CAC. When measurements were taken as a function of pH (3.0 to 12.0) and ionic strength, there was no viscoelasticity observed, indicating that the system has a synergistic polymer/surfacant interaction for surface viscoelasticity.[57] These results are comparable with those reported by Thalberg and Lindman for a sample of HA that was of higher molecular weight.[15] With HTAC/HA and TTAB/HA solutions, surface viscoelasticity occurred for those regions on the left-hand side of the phase diagram, corresponding to regions of relatively low surfactant concentration.[15] Surface viscoelasticity was shown through conductivity measurements to correspond to the regions where there is cooperative binding of the surfactant to the polymer backbone.[15]

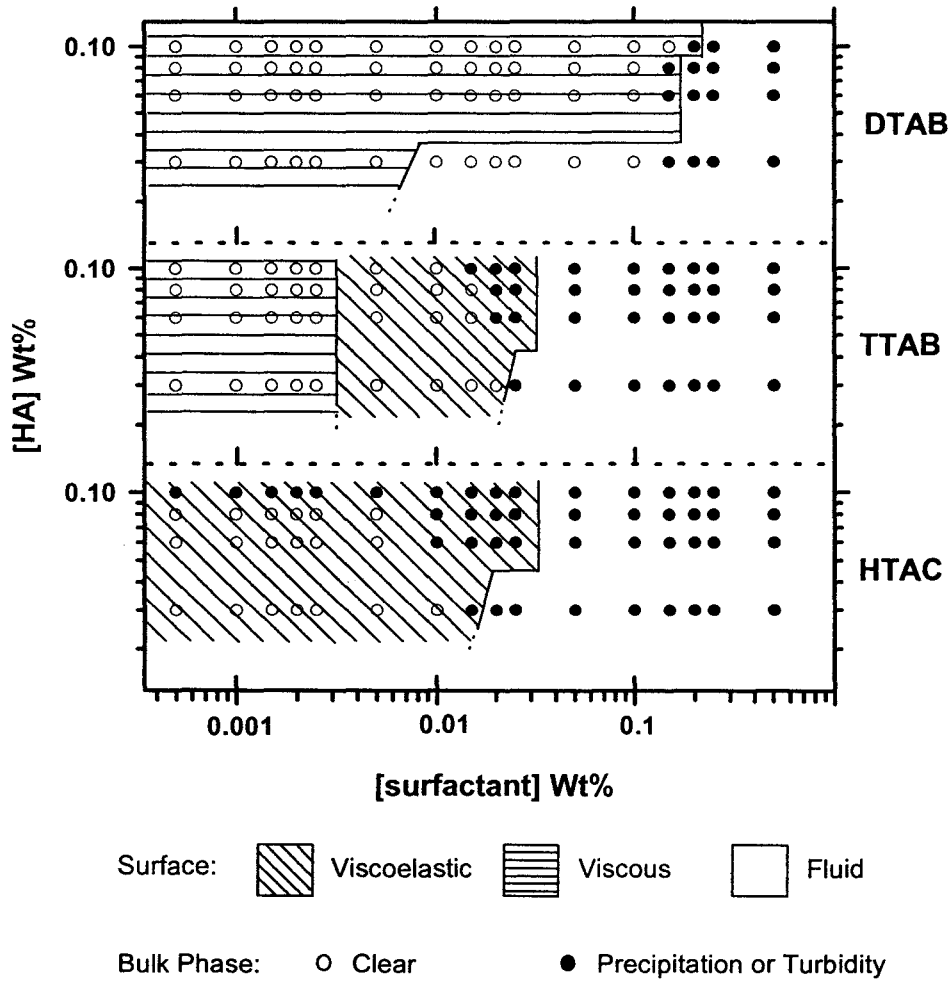

Figure 17. *Surface-phase map and solubility diagram of HA and three surfactants, HTAC, TTAB, and DTAB (pH 6.27)*[59]

4. Conclusions

To investigate the interaction of HA and amphiphilic molecules, to better understand how HA would influence cells, we have preformed a series of experiments using a variety of surfactants of varying alkyl chain length.

Using fluorescence spectroscopy solution properties for aqueous mixtures of both labeled and probed HA were investigated. HA was shown to have strong interactions with molecules of the opposite charge, namely DoPC, CPC and VEP as shown by the Stern-Volmer quenching constants.

Light scattering revealed that the HA/VEP aggregates formed increased linearly with the amount of VEP present in the system.

Surface viscoelasticity was shown to have a dependence on alkyl chain length. Surface viscoelasticity was shown for both TTAB and HTAC over a wide surfactant concentration range. However, there was only a viscous surface was shown to exist for DTAB, until at a certain concentration of surfactant fluidity was observed again.

5. Future Work

The quenching processes for EtPyBr, DoPC, CPC and VEP were found to be either static or dynamic in nature at certain quencher concentration. Therefore, performing time resolved fluorescence measurements to determine the exact quenching mechanism.

6. Appendix A

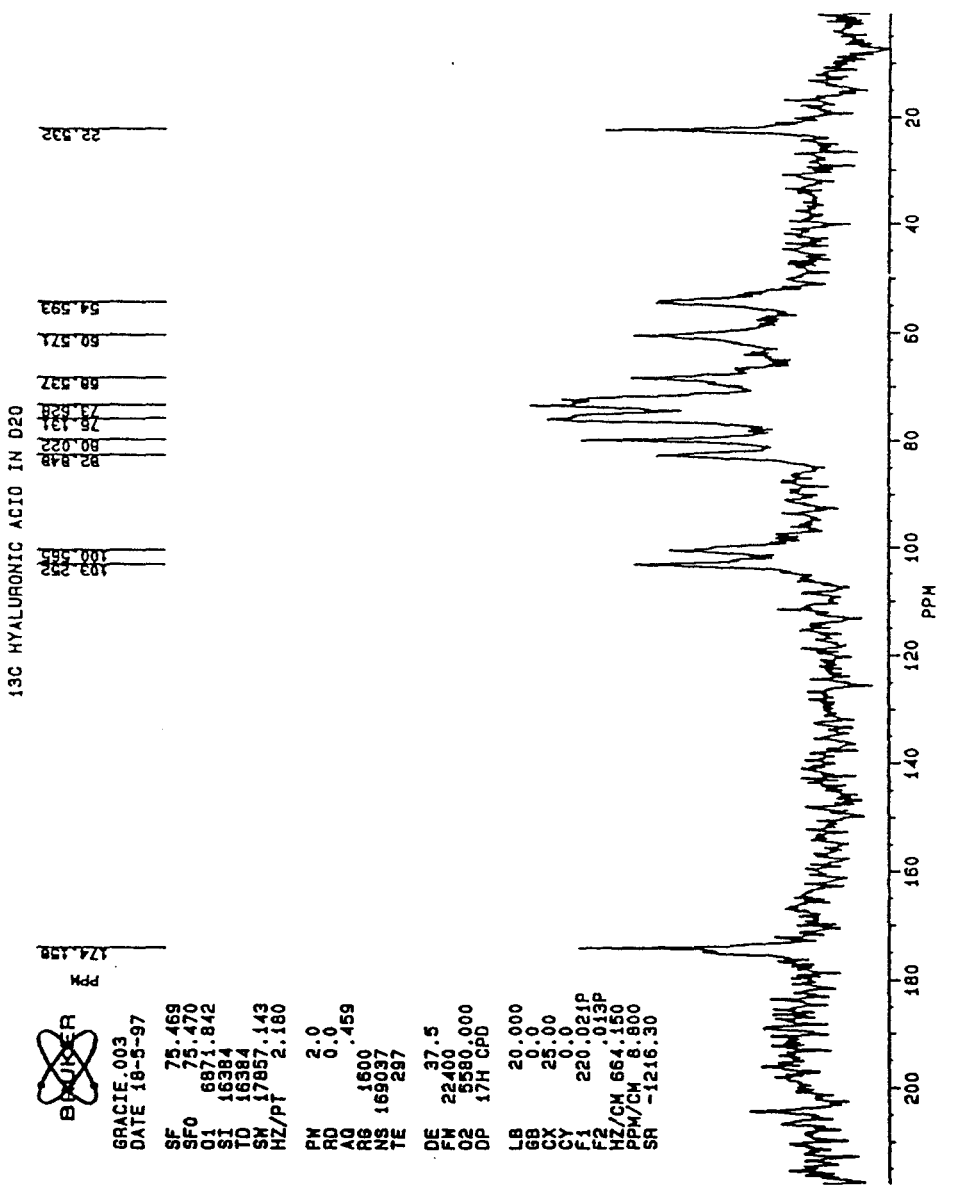

Figure 18. *^{13}C NMR spectrum of Hyaluronic Acid, obtained on AC500 MHz*

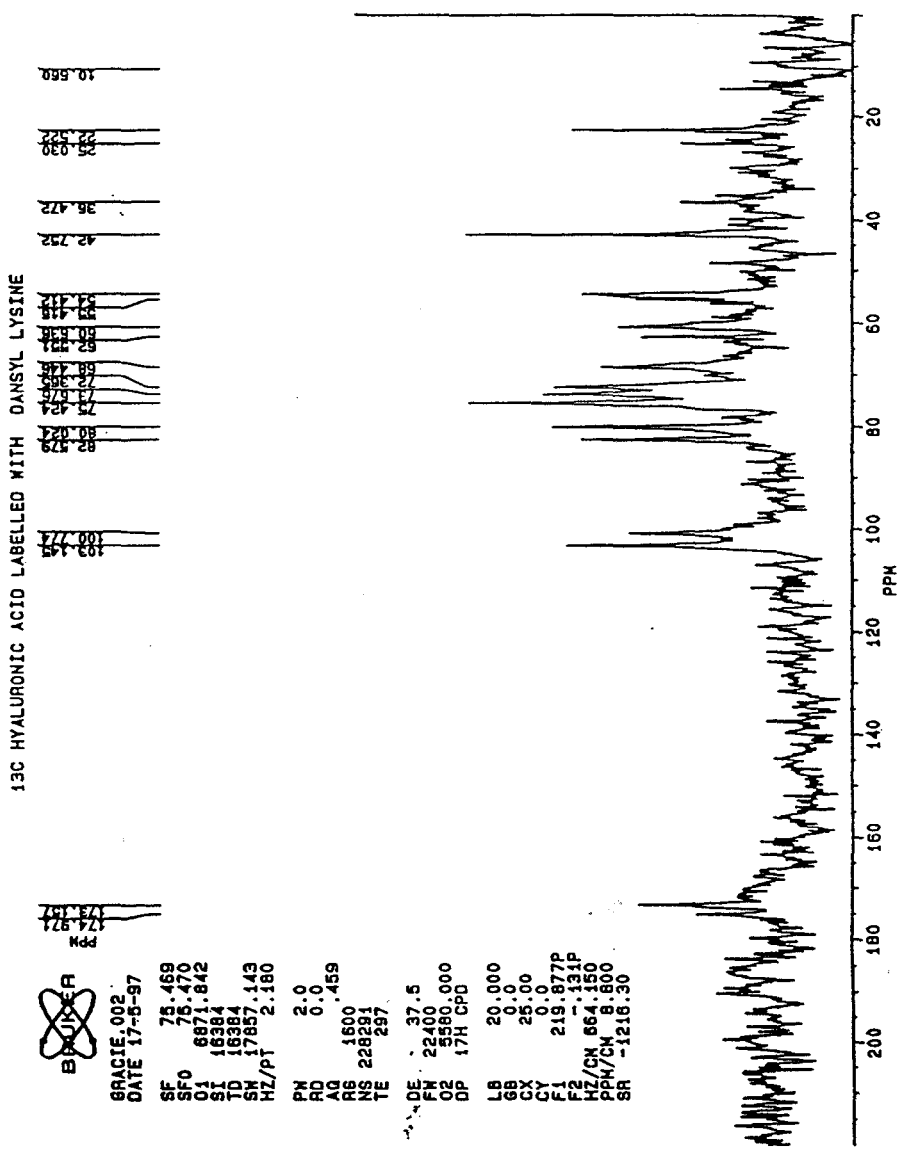

Figure 19. *^{13}C NMR spectrum of Hyaluronic Acid labeled with DL, obtained on AC500 MHz*

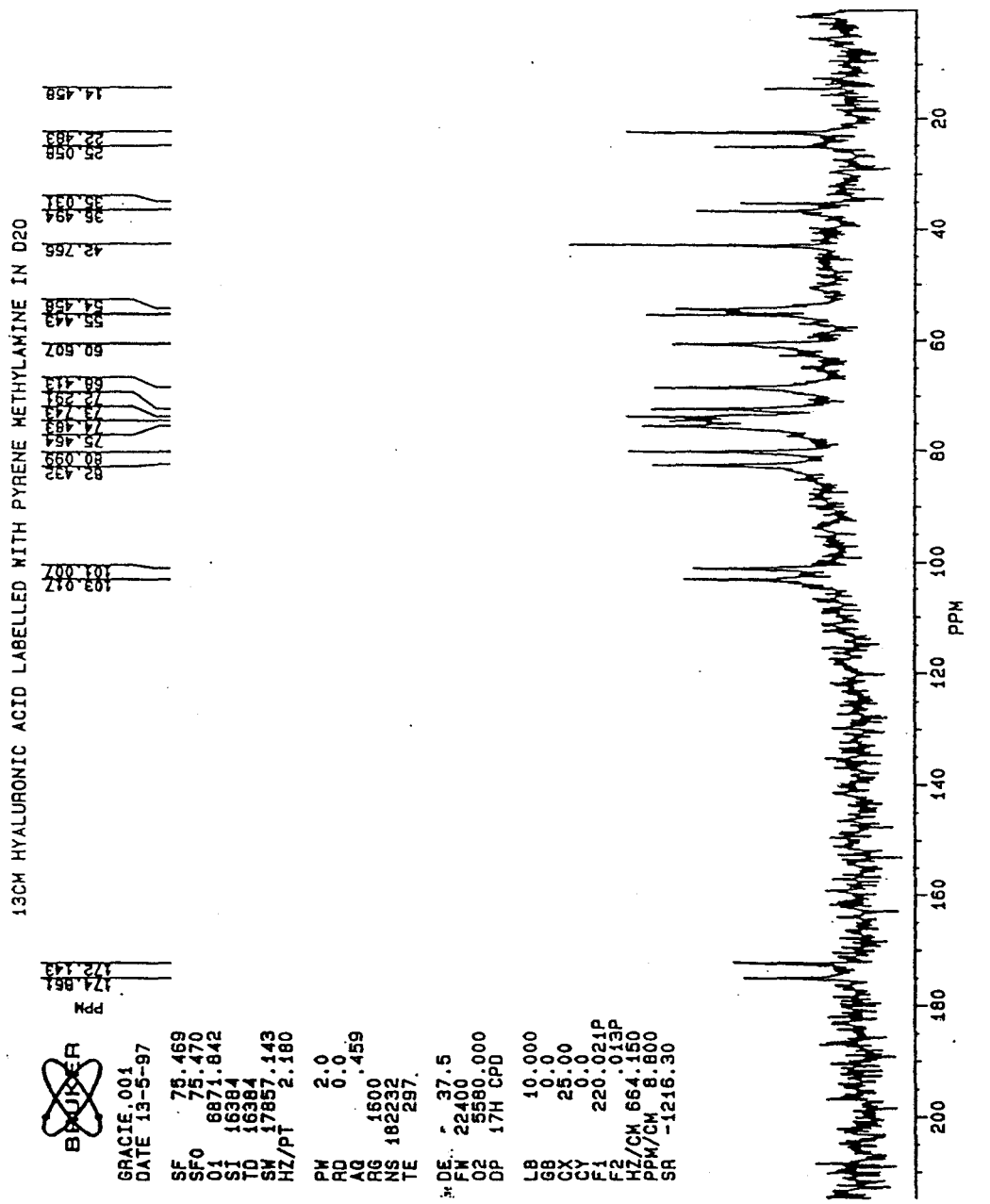

Figure 20. *^{13}C NMR spectrum of Hyaluronic Acid labeled with PMA, obtained on AC500 MHz*

7. References

1. Meyer, K. and Palmer, J.W.; *J. Biol. Chem.*; **107**, 629 (1934).

2. Scott, J.E.; Secondary structures in hyaluronan solutions: chemical and biological implications. In *The Biology of Hyaluronan,* Ciba Foundation Symposium 143, Wiley, Chichester, England, pp. 6-20, (1989).

3. Geciova, R., Flaibani, A., Delben, F., Liut, G., Urbani, R. and Cesaro, A.; *Macromolecular Chem. Phys.*, **196**, 2891 (1995).

4. Laurent, T.C. and Fraser, J.R.E.; *The FASEB Journal*, **6**, 2397 (1992).

5. Silver, F.H. and Swann, D.A.; Int. *J. Biol. Macromolecules*, **4**, 425 (1982).

6. Brimacombe, J.S. and Webber, J.M.; Mucopolysaccharides, Elsevier, Amsterdam, (1964).

7. Hayashi, K., Tsutsumi, K., Nakajima, F., Norisuye, T. and Teramoto, A.; *Macromolecules*, **28**, 3824 (1995).

8. Fumio OOsawa; Polyelectrolytes; Marcel Dekker Inc., NY, 1971.

9. Morris, E.R., Rees, D.A. and Welsh, J.E.; *J. Mol. Biol.*, **138**, 383 (1980).

10. Sheehan, J.K., Arundel, C.and Phelps, C.F.; *Int. J. Biol Macromolecules*, **5**, 222 (1983).

11. Interactions of Surfactants and Polymers; Editors, E.D. Goddard, K.P. Ananthapadmanabhan; Boca Raton, CRC Press Inc., (1993).

12. Regismond, S.T.A., Winnik, F.M. and Goddard, E.D.; *Colloids and Surfaces A: Physicochemical Eng. Aspects*, **119**, 221 (1996).

13. Winnik, F.M. and Regismond, S.T.A., *Colloids and Surfaces A: Physicochemical Eng. Aspects*, **118**, 1 (1996).

14. Fukada K., Suzuki, E., Seimiya, T.; Rheological Properties of Sodium Hyaluronate in Cationic Surfactant Solutions; Poster, OUMS Meeting (1998).

15. Thalberg, K. and Lindman, B.; *J.Phys.Chem.*, **93** (4), 1478 (1989).

16. Guilbault G.G.; Practical Fluorescence, 2nd edition, Marcel Dekker, Inc. New York, (1990).

17. Turro, N.J.; Modern Molecular Photochemisty, The Benjamin/Cummings Publishing Co., Inc., USA, (1978).

18. Li, M., Msc. Thesis; Synthesis and Characterization of Pyrene Labeled Poly(N-isopropylacrylamide-Co-N-acryloyl-L-valine) Copolymers; McMaster University, (1997).

19. Frank, R.S., MSc. Thesis; Characterization of Absorbant Polystyrene using Excimer Formation and Fluorescence Quenching Techniques, Univerisity of Waterloo, (1995).

20. Guilbault, G.G.; Practical Fluorescence; 2nd Edition, Marcel Dekker, Inc., NewYork, (1973).

21. Wehry, E.L.; Modern Fluorescence Spectroscopy 2; Plenum Press, NewYork and London, (1976).

22. Davis, G.A.; *J. Chem. Soc. Chem. Commun.*, 728, (1973).

23. Blackburn, G.M., Lockwood, G. and Solan, V.; *J. Chem. Soc. Perkin Trans. II*, 1452 (1976).

24. Hann, R.A., Rosseinsky, D.R. and White, T.P.; *J. Chem. Soc. Faraday Trans. II*, 1522, (1974).

25. Ayala, J.H., Afonso, A.M. and Gonzalez, V.; *Applied Spectroscopy*, **51**(3), 380 (1997). 26. Miola, L., Abakerli, M.F., Ginani, M.F., Filho, P.B., Toscano, V.G. and Quina, F.H.; *J. Phys. Chem.*, **87**, 4417 (1983).

26. Miola, L., Abakerli, M.F., Ginani, M.F., Filho, P.B., Toscano, V.G. and Quina, F.H.; *J. Phys. Chem.*, **87**, 4417, (1983).

27. Sapre, A.V., Rama Rao, V.S. and Rao, K.N.; *J. Phys. Chem.*, **84**, 2281 (1980).

28. Lakowicz, J.R.; Topics in Fluorescence Spectroscopy Volume 2, Principles. Plenum Press. NY, (1991).

29. Winnik, F.M., Ringsdorf, H. and Venzmer, J.; *Langmuir*, **7**, 905 (1991).

30. DeSmedt, S.C., Lauvers, A., Demeester, J., Engelborghs, Y., DeMey, G. and Du, M.; *Macromolecules*, **27**, 141 (1994).

31. Hartley, G.S., *Trans. Faraday Soc.*, **30**, 444, (1934).

32. Leezenberg, P.B. and Frank, C.W.; *Macromolecules*, **28**, 7407 (1995).

33. Garcia-Mateos, I., Perez, S., and Velazquez, M.M.; *Macromolecules*, In Print (1997).

34. Pouyani, T., Harbison, G. S. and Prestwich, G.D.; *J. Am. Chem.*, **116**, (1994)

35. Blackman, M., Lockwood, G., and Solan, V.; *J. Chem. Soc. Perkin Trans. II*, 1452 (1976).

36. Gehlen, M.H., De Schryver, F.C., Dutt, B., Van Stam, J., Boens, N., and Van der Auweraer, M.; *J. Phys. Chem.*, **99**, 14407 (1995).

37. Sinquin, A., Hubert, P., and Dellacherie, E.; *Langmuir*, **9**, (1993).

38. Winnik, F.M. and Pillai, V.; Round Table Series, **37**, 10 (1996).

39. Cowman, M.K., Hittner, D.M. and Feder-Davis, J.; *Macromolecules*, **29**, 2894 (1996).

40. Starodubtzev, S.G., Kirsh, Yu. E. and Kabanov, V.A.; *European Polymer Journal*, **10**, 739 (1974).

41. Kabanov, A.V., Bronich, T.K., Kabanov, V.A., Yu, K. and Eisenberg, A.; *Macromolecules*, **29**, 6797 (1996).

42. Bronich, T.K., Kabanov, A.V., Kabanov, V.A., Yu, K. and Eisenberg, A.; *Macromolecules*, **30**, 3519 (1997).

43. Herslöf-Björling, A., Sundelöf, L.-O., Porsch, B., Valtcheva, L. and Hjertén, S.; *Langmuir*, **12**, 4628, (1996).

44. Gracie, K.D., Turner, D. and Palepu, R.; *Can. J. Chem.*, **4-74**, 1616 (1996).

45. Pisarcik, M., Devinsky, F., and Svajdlenka, E.; *Colloids and Surfaces A: Physicochemical and Engineering Aspects*, **119**,115 (1996).

46. Silver, F.H. and Swann, D.A.; *Int. J. Biol. Macromolecules*, **4**, 425 (1982).

47. Turner, R.E., Lin, P., and Cowman, M.K.; *Archives of Biochemistry and Biophysics*, **265** (2), (1988).

48. Bonilha, J.B.S., Chlericato, G., Matins-Franchetti, S.M., Ribaldo, E.J. and Quina, H.; *J. Phys. Chem.*, **86**, 4941 (1982).

49. Ford, W., Ottwell, R.H. and Porreira, H.C.; *J. Colloid Interface Sci.*, **21**, 522, (1966).

50. Turro, N.J., Barez, B.H. and Kuo, P.-L.; *Macromolecules*, **17**, 1321, (1984).

51. Winnik, F.M., Regismond, S.T.A., and Goddard, E.D.; *Langmuir*, **13** (1), 111 (1997).

52. Winnik, F.M., Regismond, S.T.A., and Goddard, E.D.; *Colloids and Surfaces A: Physicochemical and Engineering Aspects*, **106**, 243 (1996).

53.Hann, R.A., Rosseinsky, D.R., and White, T.P.; *J. Chem. Soc. Perkin Trans. II*, 1522, (1974).

54. Herslof-Bjorling, A., Sundelof, L-O., Porsch, B., Valtcheva, L., and Hjerten, S.; *Langmuir*, **12**, (1996).

55. Eftink, M.R.; and Ghiron, C.A.; *J. Phys. Chem.*, **80** (486), (1976).

56. Eftink, M.R.; and Ghiron, C.A.; *J. Phys. Chem.*, **11**, (1976).

57. Regismond, S.T.A., Gracie, K.D., Winnik, F.M. and Goddard, E.D.; *Langmuir*, **13**, 5558 (1997).